JAERI-M
85-073

JAPANESE CONTRIBUTIONS TO IAEA INTOR WORKSHOP, PHASE TWO A, PART 2

CHAPTER I : INTRODUCTION, AND CHAPTER II : SUMMARY

July 1985

Sigeru MORI, Ken TOMABECHI, Noboru FUJISAWA, Hiromasa IIDA, Masayoshi SUGIHARA, Masahiro SEKI, Tsutomu HONDA[*1], Masao KASAI[*2] and Shin'ichi ITOH[*3]

日本原子力研究所
Japan Atomic Energy Research Institute

JAERI-Mレポートは，日本原子力研究所が不定期に公刊している研究報告書です。
入手の問合わせは，日本原子力研究所技術情報部情報資料課（〒319-11 茨城県那珂郡東海村）あて，お申しこしください。なお，このほかに財団法人原子力弘済会資料センター（〒319-11 茨城県那珂郡東海村日本原子力研究所内）で複写による実費領布をおこなっております。

JAERI-M reports are issued irregularly.
Inquiries about availability of the reports should be addressed to Information Division Department of Technical Information, Japan Atomic Energy Research Institute, Tokaimura, Naka-gun, Ibaraki-ken 319-11, Japan.

編集兼発行　日本原子力研究所
印　　刷　日青工業株式会社

JAERI-M 85-073

Japanese Contributions to IAEA INTOR Workshop, Phase Two A, Part 2 Chapter I : Introduction, and Chapter II : summary

Sigeru MORI[+1], Ken TOMABECHI[+2], Noboru FUJISAWA,
Hiromasa IIDA, Masayoshi SUGIHARA, Masahiro SEKI,
Tsutomu HONDA[*1], Masao KASAI[*2] and Shin'ichi ITOH[*3]

Department of Large Tokamak Research

Naka Fusion Research Establishment, JAERI

(Received May 31, 1985)

This report corresponds to Chapters I and II of Japanese contribution report to IAEA INTOR Workshop, Phase Two A, Part 2. The major objectives of the INTOR workshop, Phase Two A,Part 2 are to study critical technical issues, and to assess scientific and technical data bases, and to finally upgrade the INTOR design concept. To study critical technical issues that affect the feasibility or practicability of the INTOR design concept, the following five groups are organized; (A) Impurity control, (B) RF heating and current drive, (C) Transient electromagnetics, (D) Maintainability, (E) Technical benefit. In addition to those groups, the three disciplinary groups are organized to assess the worldiode scientific and technical data bases that exist now and that will exist 4-5 years to support the detailed design and construction of an INTOR-like machine, and to identify additional R&D that is required; (F) Physics, (G) Engineering, (H) Nuclear.

Keywords: INTOR, Summary, Critical Issues, Design
Tokamak, Assessment

+1 Executive Director
+2 Naka Fision Res-Establishment
*1 Toshiba Corrporation
*2 Mitsubishi Atomic Power Industries. Inc.
*3 Hitachi, Ltd.

JAERI－M　85－073

IAEA INTOR ワークショップ
フェーズ ⅡA，パート2 報告書

第Ⅰ章：序
第Ⅱ章：サマリー

日本原子力研究所 那珂研究所
臨界プラズマ研究部
森　茂[+1]・苫米地 顕[+2]・藤沢 登・飯田 浩正
杉原 正芳・関 昌弘・本多 力[*1]・笠井 雅夫[*2]
伊藤 新一[*3]

（1985年5月31日受理）

この報告書はIAEA主催のINTORワークショップ，フェーズⅡA，パート2の日本の報告書の第Ⅰ章と第Ⅱ章に相当するものである。INTORワークショップ，フェーズⅡA，パート2の主目的は重要課題を検討すること，物理と技術のデータベースを評価すること，そしてそれらをベースにしてINTORの概念設計を見直すことである。INTORの設計概念の可能性，実現性にインパクトを与える重要課題を検討するために，次の5つのグループが組織された。（A） 不純物制御，（B） RF加熱と電流駆動，（C） 非定常電磁解析，（D） 保守，（E） テクニカル・ベネフィット。これらのグループに加えて，INTOR規模の装置の設計と建設をサポートする，現在或いは近い将来に存在する物理と技術のデータベースを評価し，更に必要なR＆Dを明らかにするために，専門分野グループとして次の3つが組織された。（F） 物理，（G） エンジニアリング，（H） ニュークリア。

＋1　理事
＋2　那珂研究所付
＊1　㈱東芝
＊2　㈱三菱
＊3　㈱日立

PREFACE

This report summarizes the results of the Japanese work performed for the INTOR Workshop during the period of July 1983 through June 1985. The work has been carried out by the Japan Atomic Energy Research Institute with extensive cooperation of unversities and industries in Japan. I would like express my thanks to all of those who have contributed to the work. I would like to express also my deep acknowledgement to the IAEA and the other three parties of the INTOR Workshop for their cooperation.

June 1985

S. Mori

Executive Director
Japan Atomic Energy
Research Institute

Contents

目　　次

Chapter I : Introduction

The Workshop of the International Tokamak Reactor, INTOR, started as a collaborative effort in January 1979 among Euratom, Japan, the USA and the USSR under the auspices of the International Atomic Energy Agency, IAEA.

The initial effort called the Zero phase of the INTOR Workshop was conducted during 1979 to define the objectives and physical characteristics of the next major experiment after the existing large tokamak of TFTR, JET, JT-60 and T-15, and also to assess the technical feasibility of constructing such an experiment in around 1990. The result of the Workshop was published as the report of the Zero Phase Workshop [1]. The report concluded that an ignited D-T tokamak was technically feasible provided that supporting R&D would be properly carried out.

As a result of the Zero Phase Workshop, the INTOR Workshop was extended to the Phase One, in order to develop a conceptual design of the INTOR experiment. The Phase One Workshop completed the conceptual design in 1981, proposing a concept of tokamak having a fusion power of 620 MWt. The result of the Phase One Workshop was published in an IAEA report [2].

The INTOR Workshop was extendesd then to the Phase Two A in July 1981 to review critical technical issues which were identified during the Phase One Workshop. The Phase Two A Workshop was completed its Part I in 1983, publishing the results in an IAEA report [3].

Then, the INTOR Workshop was further extended until June 1985, in order to investigate certain technical issues that are essential to the feasibility and further improvement of the INTOR concept, to keep under review the results of the R&D programmes in various countries, and to improve the INTOR concept as a result of the new information obtained. Major technical issues addressed for investigation were;

(1) Impurity control
(2) RF heating and current drive
(3) Transient electromagnetics
(4) Maintainability
(5) Technical benefit

Extensive assessment was made on the technical data bases on the following three areas;

(1) Physics
(2) Engineering
(3) Nuclear

During this Workshop, the work has been carried out, as traditional with the INTOR Workshop, by teams of experts working in their home countries under the direction of the INTOR participants, who met in Vienna periodically. The Workshop lasted from July 1983 through June 1985.

The results of the Japanese work contributed to the INTOR Workshop during this period are contained in this national report. The work in Japan was primarily carried out by the Japan Atomic Energy Research Institute, JAERI, with the support of the industries; i.e. Toshiba Ltd., Hitachi Ltd., Mitsubishi Group and Kawasaki Heavy Industry Co., under contracts between them and the JAERI.

Many of the scientists and engineers contributed to the work in Japan were involved also in designing the Fusion Experimental Reactor, FER, a next step machine being studied at the JAERI. Thus, mamy results derived from designing the FER were conctributed also to the INTOR Workshop.

The numbering of the chapters and sections of this report was made identical as that which will be used in the IAEA Phase Two A Part II report, in order to facilitate the readers of the national report.

References:

[1] INTOR: International Tokamak Reactor - Zero Phase, IAEA, Vienna, STI/PUB/556, (1980)
[2] INTOR: International Tokamak Reactor - Phase One, IAEA, Vienna, STI/PUB/619, (1982)
[3] INTOR: International Tokamak Reactor - Phase Two A Part I, IAEA, Vienna, STI/PUB/638, (1983)

Chapter II : Summary

1. Impurity control

Physics

An INTOR core plasma produces high-energy alpha particles with their heating power, and its heat and particles flow out of a plasma core through conduction and convection with their finite confinement times. The essential objective of impurity control is to remove such large heat and particle fluxes without deteriorating plasma confinement performance. Heat and particle fluxes finally reach a first wall and a collector plate through a scrape-off plasma around the main plasma and interact with them. Critical issues for impurity control physics are, then, related strongly to the scrape-off layer property, such as parameters of scrape-off plasmas, behaviors of impurities, helium ash exhaust, basic data for surface and moleculer/atomic collisions. In an INTOR operation scenario, it is required to remove a heat flow of 124MW and a helium particle flow of around 2×10^{20}/s.

Various concepts on the impurity control have been widely assessed since the Zero Phase Workshop. Among them, the divertor concepts were evaluated to have great potential, especially the poloidal divertor was assessed to be the most promising for the INTOR impurity control. During those years, many new tokamaks went into operation and provided new useful informations, and understandings on impurity control has made great progresses. In a divertor concept, a quite new operating regime. The high-density and low-temperature divertor plasmas were observed in Doublet III experiments with a single-null poloidal configuration for the first time. Their parameters are in a quite new regime different from the past divertor plasmas, and they have several interesting features beneficial to impurity control by the divertor concept.

(1) The density in the divertor region increases nonlinearly with a density increase of the main plasma. The density near the collector plate increases to the order of 10^{20} m^{-3}.
(2) The high-density near the collector plate reduces the divertor plasma temperature there below 10eV (Fig. 1.1).
(3) Radiation losses from the divertor region also increase with changes in the density and temperature. They significantly reduce the input power to the collector plate.
(3) Along with the changes in the divertor plasma parameters, neutral hydrogen gas pressures were also observed to be remarkably enhanced.
(4) Changing magnetic configurations from limiter to divertor operation, considerable impurity reduction in the main plasmas were attained by the divertor operation. Especially, the reduction in metal impurities is observed to be remarkable.
(5) Even in NBI heated discharges, similar phenomena to Joule heating were obtained.
(6) The high-density divertor operation is compatible with the so-called H-mode discharges with good confinement time.

The high-density, low-temperature divertor plasma is caused by highly recycling particles in the divertor chamber, and the high recycling divertor concept have great advantages for impurity control. The low plasma temperature near the collector plate could results in significant reduction in

an amount of released impurity from it. The high density plasma, moreover, could be effective in avoiding penetration of released impurities from the plate. The strong radiation in the divertor chamber could also certainly ease difficulties in the heat removal of the collector plate. The pumping requirement for helium ash could also be reduced by the neutral gas compression around the divertor plasma.

From those favorable experimental results, it may be concluded that the high recycling divertor concept has some more credible features for impurity control than the conventional divertor and other impurity control concepts at present.

In order to discuss the possibility of the cold and dense divertor operation, a two dimensional program for the divertor plasma and neutral particles has been developed. The divertor plasma is strongly influenced by the neutral particles emitted from the divertor plate and traversing the divertor chamber through ionization and charge exchange reactions. Therefore, a self-consistent modelling is necessary for the description of the divertor

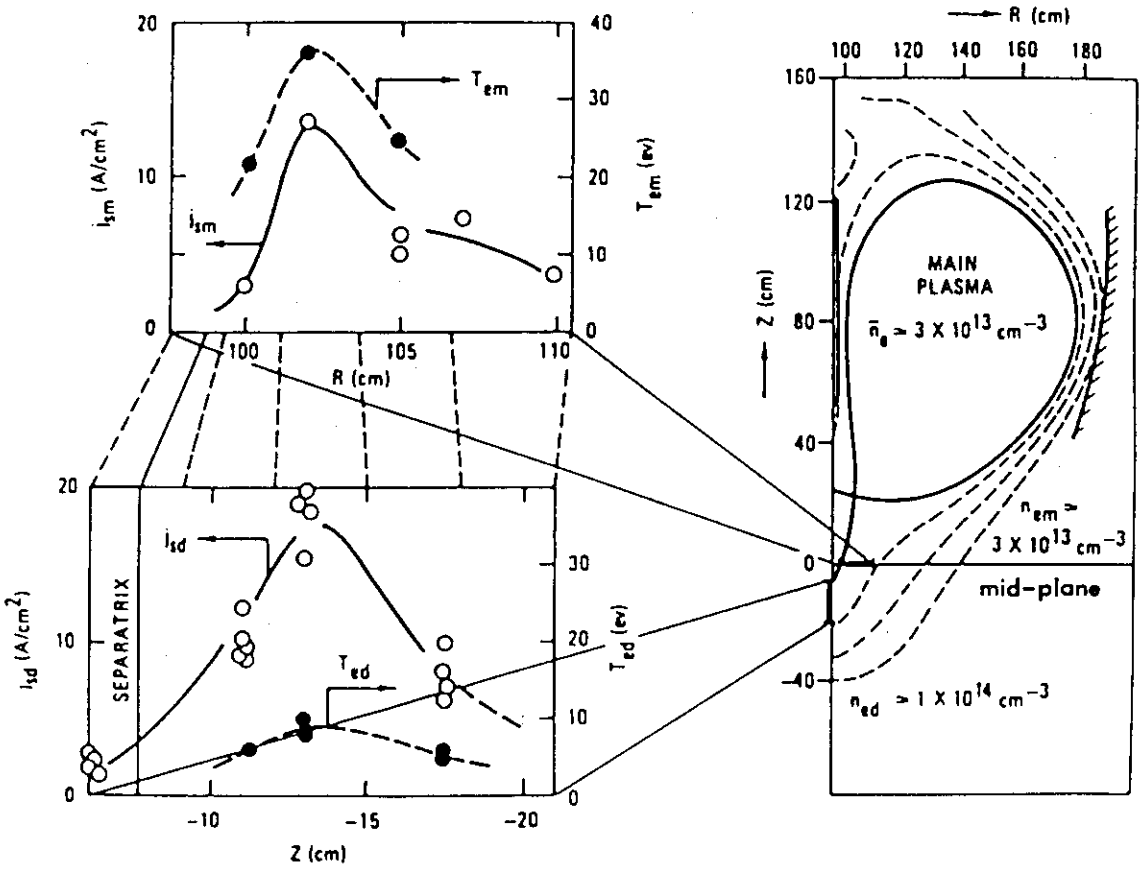

Fig. 1.1 The holizontal profile of the electron temperature, T_{em}, and ion saturation current, j_{sm}, across the lower divertor channel (mid-plane: z=0cm) and corresponding vertical profiles of T_{ed} and n_{ed} on the divertor plate at t=800ms. The connection of the field lines between both profiles is shown with dotted lines.

plasma and neutral particles. The divertor plasma is described by the fluid equations and the neutral particle transport in the divertor chamber is solved by the Monte Carlo simulation. The interactions between the divertor plasma and neutral particles are self-consistently solved by an iterative procedure.

The numerical simulation based on the above model was compared with the Doublet III experiments under 1 MW NBI heating. The main features of the D-III experiments were successfully reproduced, such as (a) formation of high density and low temperature plasmas, (b) strong radiative cooling of the divertor plasmas, and (c) nonlinear dependence of the divertor plasma density on the main plasma density.

The numerical simulation also gives the dual equilibrium solutions of the divertor plasma in the limited range of the ion flux entering the divertor. The origin of the dual solutions can be explained by a simplified modelling of the neutral particle recycling in the divertor plasma.

The divertor operating condition for INTOR was investigated based on the two dimensional program, solving consistently the divertor plasma and neutral particles. Simple analytic model is also developed to clarify the dual structure of the solution of the numerical code. The numerical results strongly suggest that the cold plasma layer less than 10 eV could be produced in front of the divertor plate, provided that the particle confinement time of the main plasma is shorter than 1.7 s (Fig. 1.2). The evaluation of the backflow fraction of the neutrals indicated the low effective pumping speed of about 2×10^4 l/s to keep the 5% concentration of the helium ash in the main plasma. When the real divertor geometry, e.g. open divertor shape, is taken into account, however, the required pumping speed should be increased up to 10^5 l/s from the parametric studies on divertor geometry. These low temperature and the required pumping speed conditions indicate that the divertor throat length could be about 50 cm and the void width be 5 - 25 cm. The sputtering erosion of the divertor plate and the other inside wall of the divertor seems not to be a serious problem, since the electron temperature could be reduced to less than 10 eV near the divertor plate.

The dependence of formation of cold and dense divertor plasmas on divertor geomeyry is studied with the simple analytic model to reduce the size of the divertor chamber. In the open geometry, cold and dense divertor plasmas are observed to be produced in a wide range of the incoming ion flux to the divertor. Temperatures at the plate become below 10 eV. The key problem of the open geometry is that the range of the incoming flux, where triple equilibrium states are observed, becomes wide. If the width of the void is retained narrow, it can be predicted that the short divertor of 50 cm length could produce cold and dense plasmas at the divertor plate. Even if the width of the gap is not so narrow, the low temperature plasmas at the plate can be obtained with some appropriate controls, such as gas fuelling into the divertor chamber.

Comparison of single and double null divertors are revisited in this phase as a possible design modification. Discussions are based on comparative studies on a national design, FER, not directly on INTOR. Those studies also include overall considerations not only from the plasma physics viewpoint, but also from the engineering aspects. Studies on the plasma physics side indicate that the double null divertor has some advantages than the single null, in areas such as the attainable beta value. Comparison is also made in

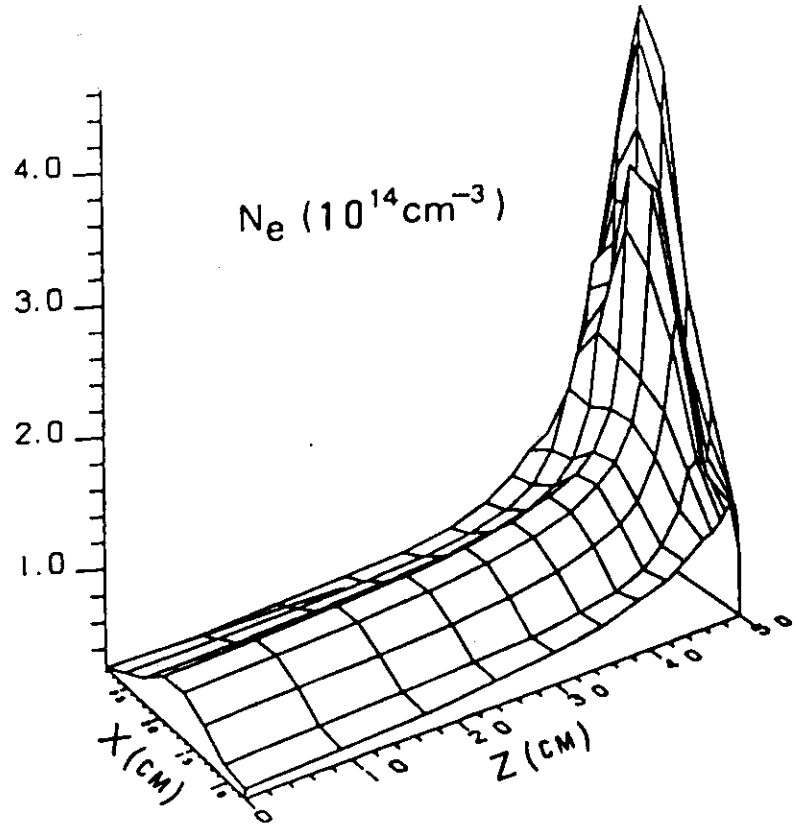

Fig. 1.2 (a) Two dimensional distribution of the electron density in the divertor plasma. (Q=40 MW, I=3x10^{22}/s)

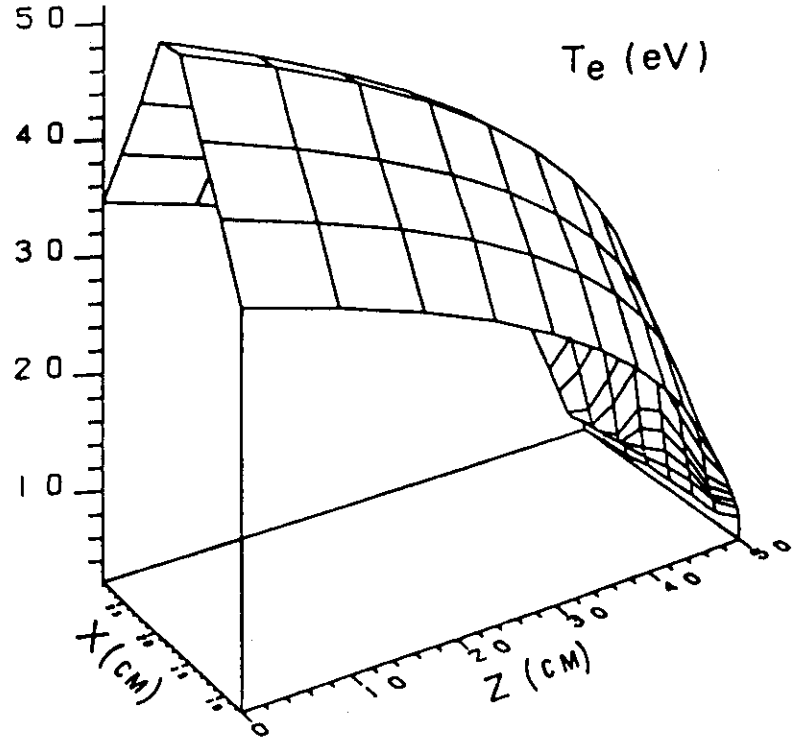

Fig. 1.2 (b) Two dimensional distribution of the electron temperature in the divertor plasma. (Q=40 MW, I=3x10^{22}/s)

engineering items, such as reactor structure, divertor collector plates, toroidal coils, poloidal coils, vertical position control, and neutronics. Those studies on engineering side show that the double null case is not favorable compared with the single. However, no definite engineering items can not be found which reasonably exclude the double null concept.

Experimental data base for limiters are also evaluated. The origin of metal impurities in tokamaks is generally considered to be due to three different types of wall interaction, i.e. arcing, evaporation and sputtering.

Arcing phenomena are observed to occur on the first wall in nonequiliblium phases such as the current rise and shut down phases as well as plasma disruption. The most probable cause of unipolar arcing in tokamaks is that run away electrons increase the sheath potential between the wall surfaces and the non-equiliblium dense plasma in the scrape-off plasma, and produce the arcs. Unipolar arcing will hardly occur during the steady state even in future large tokamaks, if the first wall is well conditioned and the heat flux to the wall is kept below 500 W/cm^2. Evaporation due to the heat flux from the plasma does not constitute a mechanism of metal impurity production in normal discharges.

Sputtering is the dominant process in the steady state of the tokamak operation. To reduce the amount of metal impurities released from the wall by sputtering, temperatures and charge number of ions in the scrape-off plasma must be kept low. Metal impurity can be reduced by Ti gettering, gas puffing and use of graphite limiter

By using a centrifuge pellet injectors as the principal D_2 fueling source, good confinement and high density plasmas have been obtained in the neutral beam injection heating of Doublet III tokamak with limiters. The neutral pressure at the upper chamber and the particle recycling at the limiter surface, as infered from the D_2 emission level, for pellet fueled discharges are two to three times lower than those of gas fueled discharges. The global energy confinement time obtained by diamagnetic measurement degrades in beam heated gas fueled discharges as observed generally in present tokamaks. The confinement time is improved 1.7 times by central fueling (pellet fueling) compared peripheral fueling (gas fueling) discharges at 2.4 MW of beam power, however degrades with increasing the beam power corresponding to decreasing the pellet penetration.

Particle and energy fluxes in the scrape-off layer behind the limiter have been studied in the JFT-2 tokamak. The diffusion coefficient of the scrape-off plasma is the order of the Bohm diffusion coefficient. The total heat flux density to the rail limiter during a discharge are compared between the electron and ion sides of the limiter. This indicates the higher heat flux on the electron side is mainly due to accelerated electrons. In order to reduce the heat flux to the limiter, it is important to operate the higher density.

We performed a detailed recycling calculations of neutral particles on the limiter and the first wall with the aids of the one-dimensional tokamak transport code. The energy of neutral particles flowing back from the limiter chamber and the necessary pumping speed to realize the recycling rate used in the one-dimensional transport code are calculated by the two-dimensional Monte-Carlo neutral code independently. The feasibility of the pumped-limiter

were analysed. The electron temperature in the scrape-off layer decays in radial direction toward the wall very rapidly with the characteristic decay length of about 1 cm, while the density distribution is slightly broad. When a rather short limiter is installed, moderate pumping system is sufficient to keep the helium accumulation in the main plasma at the desired level. The electron temperature at the separatrix is about 400 eV when the realistic pellet injection by the present-day technology is employed. It will be difficult to further lower the temperature without increasing the helium accumulation level. Fueling by gas puffing gives almost the same results. To solve the high heat flux and erosion of the pumped limiter, cool boundary plasma may be indispensable. This cool boundary plasma must be restricted to the periphery and the hot core plasma must be unaffected by it to sustain the self-ignition state.

Ergodic limiters and rf pumpout are numerically studied as innovative schemes of the impurity control. The ergodic magnetic layer produced in the periphery of the tokamak plasma by subsidiary helical currents (Ergodic Magnetic Limiter) can be effective for equalizing the heat load on the first wall. In order to examine the possibilities of these concepts we numerically analysed the formation and destruction of the magnetic islands produced by resonant helical currents. Calculations on a single set of double $l=3$, $n=1$ helical coils with same constant current in opposite directions show that the magnetic surfaces outsides the $q=3$ surface are effectively destructed, when the value of helical currents is larger than a critical value which is very small compared to the plasma current. The effect of the local helical coils is also examined which were wound in the localized regions along the toroidal direction of the torus, because they are of greater practical use from the engineering viewpoints. It is observed that the magnetic islands also rotate in this case, although about five times larger current are needed than the case of full windings.

The active control of impurities requires some additional input of momentum (energy) into a plasma. The use of radio-frequency (RF) wave momentum has recently been proposed. This is called RF divertor where waves are launched into a plasma by external RF generator in the ion-cyclotron range of frequencies. Those impurity control schemes, ergodic limiters and rf pumpout, have little experimantal data base, then further experimental studies are required.

Recent experiments indicate that fueling physics is deeply correlated with plasma confinement property. Discharges without degradation of a confinement time during NBI heating, the so-called H-mode, are found to be strongly influenced by the fueling and recycling at a plasma edge. Remarkable improvement in a confinement time of limiter discharges are lately observed in Doublet III by using a pellet injection. The confinement time of discharges with a limiter is significantly improved by the deep penetration of the pellet and reach the almost same value of the H-mode discharges with a divertor. The results indicate importance of the low recycling in the edge plasma and is consistent with the feature of the H-mode discharges.

Data compilation and evaluation for atomic and molecular processes and for plasma-surface interactions is being in progress. Those activities include the atomic structure data of Fe ions, the charge transfer cross sections of ions in collisions with atomic and molecular hydrogens, excitation cross sections and rate coefficients in electron impact for carbon and oxygen

ions in various ionization stages, the ionization cross sections of ions by electron impact, atomic processes in hot, dense plasmas and on ion-ion collisions. The importance of understanding behavior of low temperature plasmas near the edges, limiters and divertors urged us to compile data involving the ionization of neutral atoms and excitation, dissociation and recombination processes of atomic and molecular hydrogen atoms/ions. Compilation and evaluation of sputtering data by ion impact have been completed for monatomic solid targets. The incident energy dependence, angular distribution and incident angle dependence of total sputtering yields have been evaluated and some empirical formulas for sputtering yields have been found. Data for the particle- and energy-backscattering coefficients are compiled and evaluated and empirical formulas for these data in normal and oblique incidences have been found. In order to make easy access to the bibliographic and numerical data, a computer-based data storage and retrieval system has been developed. The databases developed by ourselves as well as those commercial and exchanged with other data centers are available. These data can be retrieved through TSS or telephone line linkage.

For the last five years, the data base on surface effects related to impurity production has been extensively produced and compiled both experimentally and theoretically. They include hydrogen chemical sputtering yields of low-Z materials such as C, SiC and TiC in the energy range between 0.1 and 6 keV, their surface compositional changes by bombardment with energetic hydrogens, energy dependence of the hydrogen chemical sputtering of carbon materials and their theoretical model, chemical erosion of graphite by atomic hydrogen exposure, chemical erosion by oxygen ion bombardment of refractory metals such as W and Mo, energy dependence of self sputtering yields of W and Mo at room temperature in the energy range between 0.1 and 10 keV, an empirical formula for the energy dependence of physical sputtering yield of monatomic solids. As far as surface effects related to particle recycling are concerned, the following items are studied experimentally and theoretically, such as hydrogen recycling model at wall surfaces in tokamaks, hydrogen diffusivity data on Ni and Mo, an effect of radiation damage on deuteron re-emission and trapping, deuterium re-emission measurement during energetic deuteron bombardment in Mo, Inconel 625 and TiC, ion-induced release of deuterium from Mo by low energy proton bombardment at room temperature, empirical formulas of light ion backscattering coefficient for both particle and energy as a function of incident energy

Data on vacuum vessel preparation are also assessed. It includes experiments on electron cyclotron resonance (ECR) discharge cleaning on JFT-2, JIPP T-II and TEXTOR, which has been proved that the vacuum components between the liner and vacuum vessel can be cleaned by this method, a carbon wall experiment on DIVA in which once clean surface was obtained by discharge cleaning very low q plasmas with a good confinement characteristic were maintained for several hundreds shots without any additional cleaning procedure, a special stainless steel doped with boron (0.01 %) and nitrogen (0.16 %) heated to about 800 °C in vacuum, where a very thin layer of hexagonal boron nitride is formed on the surface, a hard and anti-corrosive titanium nitride coating proposed for use as a protective coating for the inside of vacuum vessels, development of surface coatings of low-Z materials for JT-60, investigation and testing of materials and methods for attaining to low outgassing rates without bakeout.

(Engineering)

In the course of the Phase 2A, Part 2 sessions, our efforts have been mainly devoted to "Low Edge Temperature Divertor Design," and "Data Base Assessment".

Design studies of the divertor collector plate were made for the high recycling and low particle temperature operating conditions. The conditions are quite attractive for the engineering design, since little or no sputtering erosion is predicted for high-Z materials at low edge temperatures. The studies included material considerations, configuration, thermo-hydraulic and stress analyses, disruption, lifetime analyses, and tritium permeation.

The divertor collector plates consist of a water cooled copper or copper alloy heat sink which is protected by a tungsten tile bonded to the surface. Two divertor configurations were considered. One is essentially unchanged from the previous INTOR configuration. The heat flux on the inner collector plate was 5 MW/m^2. The other is the one where the plate is further inclinded to limit the surface heat flux less than 2 MW/m^2. Tungsten tile thickness was taken to be either 1 mm or 3 mm. The effect of bonding methods on the mechanical characteristics of tungsten and copper were discussed.

Thermo-hydraulic and stress analyses were also made for the collector plate with a thin stainless steel layer on it.

Thermal response, melt layer depth, and evaporated thickness due to a plasma disruption were calculated for the tungsten tile covered by a thin stainless steel layer. The situation simulates the case where the stainless steel sputtered at the first wall accumulates on the divertor surface. Stability of the melt layer was analytically treated with the aid of hydrodynamic linear stability theory.

In addition to the studies of the low edge temperature divertor, trade-off studies were made to examine the use of helium gas coolant for the first wall, and the advantages of long pulse operation.

The major conclusions and recommendations are summerized as follows:

(A) Low edge temperature divertor

1) The geometry of the divertor plate and the divertor chamber depends on the plasma configuration (the magnetic field lines). Two plasma configurations have been considered for the engineering study. The first plasma configuration is the same as the Phase I design. The second plasma configuration is based upon the Japanese physics prediction. More physics information is neede to establish the best solution of the divertor geometry.
2) Under the Phase I divertor configuration, the maximum heat flux is 7 MW/m^2 on the inner plate. The maximum heat flux is reduced to 5 MW/m^2, if the inner plate is placed at an angle of 20° to the field lines. The other divertor configuration has been considered in order to limit the peak heat flux to about 2 MW/m^2. The angle between the divertor plate and the separatrix is 8° for the inner channel, and 6° for the outer channel.
3) The divertor chambers for the long channel length divertor and the reduced channel length divertor have been compared. The length of divertor channel has been taken to be 40 cm for the reduced channel length divertor. The peak heat flux has been taken to be either 5 MW/m^2 or 7 MW/m^2 fot both long and reduced

channel length divertor. The reduced channel length divertor gives the decrease of 0.45 to 0.6 m in the height of divertor chamber compared with the long channel length divertor.

4) The divertor collector plate is composed of a protective material, heat sink, and supporting structure. The protective material is 1 mm or 3 mm thick tungsten. The heat sink is pure copper or a copper alloy, and the support structure is stainless steel. The protective tile is brazed or plasma-sprayed to the heat sink.
5) Stress and fatigue analyses of the divertor plate indicate that the peak heat flux less than 2 MW/m^2 is required to reduce the thermal fatigue stress range to an acceptable level. An unacceptably short lifetime results under the peak heat flux of 5 MW/M^2. The plasma spraying is preferred to the brazing from the standpoint of heat sink fatigue life. However, the strength and fatigue life of tungsten appear to be critical for the plasma spraying.
6) The stress in the divertor plate is quite sensitive to the deposition thickness of 316 SS. The stress increases with increasing the deposition thickness. Deposition of 316 SS on the divertor plate could result in significantly reduced life.
7) The bulk mechanical property data base for the protective material and the heat sink is small, and there are greates uncertainties in the interface bond strength. Further studies are needed for the accurate lifetime estimation and the selection of reference bonding method.

(B) Additional studies

8) The first wall is composed of Type 316 stainless steel. If the melt layer is stable, the thickness with an allowance for erosion of first wall is only 6.9 mm, and the first wall is expected to survive the reactor lifetime in terms of fatigue damage accumulation. Using the assumption that the entire melt layer is lost, the first wall has to be replaced at least once.
9) Thermo-hydraulic analyses were made on a helium-cooled first wall. The results indicate that a practical design of the first wall is possible with helium coolant.
10) Thermal response of the divertor plate covered with thin stainless steel layer were calculated for the reference disruption energy flux of 230 J/cm^2 with the duration of 5 ms or 20 ms.
    i) Tungsten does not melt for either of the conditions.
    ii) Melt layer and vaporized thicknesses increase with increasing thickness of the stainless steel.
    iii) In the case of 1 m deposition layer, the SS layer completely melts for 5 ms disruption. Thus if all the melt layer is lost, stainless steel cannot accumulate on the tungsten surface thicker than 1 m.
    iv) Judgin from these results, a certain deposited thickness exists which melts completely for 20 ms disruption.
11) Melt layer stability was analysed with the aid of the hydrodynamic linear stability theory. As long as the theory is applicable, the melt layer is predicted to be unstable. Further studies are required.

12) The first wall is composed of Type 316 stainless steel. If the melt layer is stable, the thickness with an allowance for erosion of the first wall is only 6.9 mm, and the first wall is expected to survive the reactor lifetime in terms of fatigue damage accumulation. Using the assumption that the entire melt layer is lost, the first wall has to be replaced at least once.

13) The lifetime of the divertor plate and the first wall has been analysed for the long pulse operation, and has been compared with that in the reference operation. The advantages of the long pulse operation are:
   i) The fatigue life of the divertor plate is 5 times longer than that in the reference operation. For the long pulse operation, the fatigue life of heat sink is 3.3 year in the Case 1, and 1.6 year in the Case 2.
   ii) The lifetime of the first wall is expected to be more than the full reactor lifetime. On the other hand, it would be necessary to exchange the first wall at least once for the reference operation of Case 2.

14) The limiter is composed of either Be or C bonded to Cu heat sink and support structural material (316 SS: 40 mm thick). 3-D thermomechanical calculations were performed for four cases of 10/20 mm thick Be and 5/10 mm thick C. The stress intensity in the Cu heat sink is below the 3Sm limit for all cases.

15) The lifetime considerations for the limiter plate were made in terms of the erosion and gatigue. The conclusions are that:
   i) the Be-Cu and C-Cu limiter plates are expected to survive the reactor lifetime in terms of fatigue damage accumulation,
   ii) the consideration of the erosion results in an unacceptably short lifetime, at most 0.1 y in the case of 20 mm thick Be, and
   iii) further analysis should be made with consideration of the erosion/redeposition for the leading edge.

2. RF Heating and Current Drive

Data base assessments of bulk heating for ion cyclotron range of frequency (ICRF), for lower hybrid range of frequency (LHRF) and for electron cyclotron range of frequency (ECRF) were performed. Assessments of current drive for LHRF and of start-up assist by ECRF were also undertaken.

2.1 Ion cyclotron waves

Major ICRF heating experiments are now in progress on JFT-2M (JAERI), JIPPT-II-U (Nagoya) and Heliotron-E (Kyoto). Before these, ICRF heating experiments were carried out in DIVA (Prf - 100 kW, 1978 - 1979) and JFT-2 (Prf - 500 kW, 1981 - 1982) of JAERI and JIPPT-II (Prf - 300 kW, 1981 - 1982) of Nagoya. Heating regimes used in the ICRF heating experiments cover the two-ion hybrid (D-(H), D(^{3}He), ( ) denotes minority component), the second harmonic (pure H), the ion Bernstein wave (H(^{4}He)) and the slow (ion cyclotron) wave (Pure H). The two-ion hybrid regime is employed most commonly and its heating efficiency is $3.7 - 6.6 \times 10^{19}$ keV/MW$\cdot$m^3. It was demonstrated in JFT-2 experiment, where a launching structure was located on the high field side, that power partitioning among species changes with n_H/n_D, i.e. D majority heating ($n_H/n_D = 2\sim4\%$) H minority heating ($n_H/n_D \approx 10\%$) electron heating ($n_H/n_D \approx 30\%$). The second harmonic heating was investigated in JFT-2M and Heliotron E. The second harmonic heating was successful only when the target plasma was heated by neutral beam injection (NBI) in JFT-2M. This fact indicates that the second harmonic heating is suitable for high temperature and high beta plasma, which is consistent with theoretical prediction. The heating efficiency of 4.3×10^{19} keV/MW$\cdot$m^3 can be obtained. The efficiency of Heliotron E is 3.3×10^{19} keV/MW$\cdot$m^3. Ion Bernstein wave heating is investigated in JIPP T-IIU. The heating efficiency is comparable to that in two-ion hybrid regime.

In these experiments conventional loop antenna with Faraday shield are used. Coupling efficiency of 50 - 90% was obtained. Parametric dependences of the antenna loading resistance on plasma parameters are well explained with calculation quantitatively.

Considerable progress was also made in the theoretical modelling of ICRF heating. The method of solving a wave equation as a stationary boundary-value problem is used since the typical wavelength in a tokamak becomes comparable with the dimension of the device in the range of ion cyclotron frequency and the ray tracing method fails the validity. Three different codes, kinetic one-dimensional, cold two-dimensional and kinetic two-dimensional codes, have been developed to include realistic geometory. Numerical results well explain the tendency of the experiments.

INTOR bulk plasma heating system using ICRF requires 60 MW of injection power to reach the ignition and heating time for the ignition is 6 seconds. ICRF launcher constructed till now are basically devoted to study a heating principle, so that the RF systems are of low power, short pulse and low duty factor. Certain extension of current state-of-the-art will be required to manufacture RF-coupling antenna, feed-through, transmission lines and power source. Wave coupling mechanism has been adequately comprehended. However some problems are remained to be solved: the first is the allowed sparsity degree of Faraday screen plates. The second is the plasma effect to the voltage breakdown in the loop coupler. An intense R and D program will be necessary to develop ICRF heating to the level required for INTOR.

The choice between RF waves for bulk heating in INTOR, at present, rests on a trade-off between the engineering and technical advantages of RF heating. From the data base assessments, the ICRF can be the first candidate. In the ICRF, we can also conclude that the $2\omega_{CD}$ heating of INTOR plasma is feasible, but some other back-up heating is necessary in the initial stage of the heating. Furthermore, it is also important for INTOR that impurity influx is significantly reduced by control of $k_{\parallel}$ spectrum of an antenna array. This is a strong experimental evidence of the merit of the 2×2 antenna array proposed for INTOR. The feasibility of the $2\omega_{CD}$ heating and the 2×2 loop antenna array will be tested with a reactor-grade plasma of JT-60 in the near future.

2.2 Lower hyrbid waves

LHRF heating was successfully demonstrated in many tokamaks. Efficiency in the ion heating mode ($\leq 4 \times 10^{19}$ eV/kW$\cdot$m^3 in JFT-2, JIPP-TII, Petula) become comparable to those of ICRF and NBI ($\leq 6 \times 10^{19}$ eV/kW$\cdot$m^3 but still less effective. The key point to improve the efficiency is the understanding of the surface phenomena like parametric instabilities etc. On the other hand, the efficiency of the electron heating mode is excellent ($10 - 20 \times 10^{19}$ eV/kW$\cdot$m^3 in FT, Alcator-c) where decay waves were scarecely observed. But electron heating mode requires higher toroidal field ($\geq$ 6 T) and higher frequency ($\geq$ 3 GHz) in INTOR.

Efficiencies of the both heating modes are adequate for the ignition of the INTOR plasma with practical power level. Technology of the RF generator and coupling structure required for the INTOR is within the extension of the present level. Therefore, it is recommended to prepare the LHRF heating in INTOR. Final decision of which is better, ICRF or LHRF, should be done after the ongoing program in JT-60, FT-U and Tore Supra, etc.

Another important role of LHRF is current drive. Almost all of the present data base for the current drive is restricted to the low density plasma. In the low density discharge, many experiments, where the plasma current is ramped up with various combinations of LH current drive and OH coils have been carried out. For example, it has been verified in PLT that the plasma current driven by OH coils is sustained with LH current drive. It has been performed in PLT, JIPP-TIIU, WT-2 etc, where the plasma current is initiated and ramped-up without OH coils but with LH current drive. Furthermore, it has been demonstrated that the plasma current can be driven by LH wave under the inverse DC electric field in PLT.

Figure of merit of current start up $M = I_{RF}R/P_{RF} \sim 3$ MA$\cdot$m/MW$\cdot$s. Current drive efficiency $\eta = n(10^{19}\ m^{-3})\ I_{RF}(MA)\ R(m)/P_{RF}(MW)$ were ~1 in JFT-2M, 0.6 in JIPP-TIIU and 0.06 in WT-2. The efficiency η increases with plasma current (JFT-2M). Hence, the power required for the steady state operation of INTOR is ~300 MW and it should be premature to employ the complete steady operation scenario with the use of lower hybrid current drive (LHCD) in the burning phase. If the effifiency is improved by factor 3, it is the best scheme for the tokamak operation. From present status of these experiments, LHCD in low density plasma have exploited the operation scenario — plasma current ramp-up and sustainment of plasma current during transformer recharging (quasi-steady operation). Although the specification of LHRF wave for LHCD to realize the quasi-steady operation has not fully identified yet, preliminary evaluation shows that 10 ~ 20 MW of power is needed for this purpose. Broad wave spectrum is predicted to be necessary to drive sufficient current. Rather low ave frequency many be preferable due to low

reflection coefficient of the wave at the plasma periphery.

If the plasma current can be successfully ramped-up by LH in the present device, the burn time will be prolonged to 1500 ~ 2000 seconds. On the other hand, of the burn time is set to the order of the resistive skin time t_{sk} (300 ~ 500 seconds), the major radius could be reduced by about 1 m. The burn time of the order of t_{sk} will be necessary and sufficient for the physics experiments of the inductive current drive. Although the samll reactor size may be attractive, any burning experiments should be failed if the sufficient current ramp-up by LH is failed. In addition, the demonstration of stable longer burn of about 1500 ~ 2000 seconds would be useful and important for the future possibility of inductively driven commercial reactor. Based on the above discussions, we propose a following scenario for INTOR. (1) Burn time should be prolonged at least to the order of t_{sk} by LH current drive. In addition, longer burn time (1500 ~ 2000 seconds) should be included in the target of the experiments. (2) Quasi-steady operation should also be included in the target no matter how the burn time is, since this operation scenario will bring about the engineering merits in INTOR.

2.3 Electron cyclotron waves

Electron Cyclotron Heating (ECH) is considered to be an important method by which all of the processes such as preionization, start-up, heating, current drive and profile control of the plasma are possible in principle.

In the JFT-2 tokamak, three types of the fundamental (n = 1, 28 GHz) modes were launched, i.e. X-mode from inside, O-mode from outside and TE_{02} mode(which is the direct output of the 200 KW gyrotron) from the top, and compared. The oblique launch of the X-mode gave the most efficient heating (efficiency $\eta \geq 90\%$) in consistent with the theoretical prediction. Increase of the T_{eo} from 600 eV to 1250 eV in the peaked profile was observed. In the JIPP T-II stellarator, 40 KW of 35.5 GHz microwave power was injected. Both O- and X-mode (n = 1) were launched from outside in the circular TE_{11} mode. The same heating efficiency of 2.2×10^{19} eV/kW·m^3 at $\bar{n}_e = 6.0 \times 10^{19}$ m^{-3} was observed. In the fundamental resonance of Heliotron E, total kinetic energy increased with the density and the maximum value was obtained near the cutoff density of the O mode. The maximum heating efficiency of 6.5×10^{19} eV/kW·m^3 was observed. In WT-2, the ECR-plasma with $\bar{n}_e = 2 \times 10^{18}$ m^{-3} was generated and there appeared a week plasma current $I_p \simeq 0.5$ kA.

In INTOR, frequency of the wave is 140 GHz and injection power of about 5 MW seems sufficient for the start up assist, while injection power of about 10 MW may be required for 10 seconds. Since the first experiment, the pump frequency has been raised step by step and 86 GHz is the highest frequency available now. The cut off density of this frequency is $n_c = 0.9 \times 10^{20}$ m^{-3}, and heating of the thermonuclear core plasma is possible by ECH. However, the developments of a high frequency and long pulse gyrotron, and a transmission system are necessary. In conclusion, ECH system, especially, for preionization, startup and profile control of the plasma, which can be done within the extension of the present power level, should be prepared in INTOR.

2.4 Other methods for heating and/or current drive

There are many useful methods for plasma heating and/or current drive except ion cyclotron, lower hyrbid and electron cyclotron waves. One of them is turbulent heating. TRIAM-1 tokamak plasma is turbulently heat by inducing pulsive toroidal plasma current. If we adopt the

turbulent heating in the INTOR tokamak, we can expect effective ion heating. But we must apply much higher voltage to the turbulent heating coil.

Another method is relativistic electron beam (REB). In SPAC-VII, REB ring current continuously increased during the long pulse injection. The rate of the current rise was $2-4\times10^{4}$ MA/sec at the injection current of 30 kA. This result suggests that there is a possibility of the use of electron beam injection for start-up or sustainment of tokamak currents. However, it should be noted that electron beam injection into the deep inside of a large current column might be difficult unless a proper mechanism is present. For practical application of this electron injection to large tokamaks like INTOR, much more study is necessary.

3. Transient electromagnetics

The purpose of this section is to provide a summary of the work of the Chapter 5 "transient electromagnetics" carried out for INTOR workshop phase 2A (part 2) during FY 1984. Parametric studies are carried out for both JAERI FER '84 and INTOR. An overview of the key results are presented in the rest of this section.

Plasma stabilization

The stabilizing properties of passive elements and the effect of plasma model are surveyed for plasma vertical position control. The effects of the number of conductive shell segments, inboard conductive shells and shell thickness are analized for the FER. Table 3.1 summarizes the results of this parametric study. The growth time of vertical position instability is approximately in proportion to the reverse of the number of segments.

Based on this study, two conductive shell designs are selected for simulation study on feedback control of plasma vertical position. The fesults of the simulation study are summarized in Table 3.2. The power supply capacity of 30~50 MVA will be required when active coils are installed outside toroidal field coils. The error and delay time in position detector and the dead time of thyristor do not strongly affect the power supply requirement and maximum displacement within the range of our survey if the growth time of conductive shells is high enougth The power supply requirement dose not strongly depend on the shell structure but on the active coil location. On the other hand, the maximum plasma displacement is affected by the shell structure. Parametric studies are also performed for the INTOR plasma.

Preliminary study on plasma radial position control are carried out by simulating plasma movement at disruptions. Impractically large power is required to recover the plasma radial position.

Start-up effects

The shielding properties of passive structures against magnetic field and electric field are analized for the FER. The vacuum vessel without bellows (high one turn toroidal resistance) prevent the penetration of the magnetic field by active coils when active coils are located outside toroidal field coils. So untolerably large power would be required for plasma position control in the system with no bellow and outer active coils. As a function of bellows resistance, figure 3.1 shows the time evolution of plasma loop voltage normalized by the loop voltage without any passive structure surrounding plasma. One turn troidal resistance of ~0.2m is reasonable, if plasma current is ramped up by inductive method.

Plasma disruption effects

The induced voltage and electromagnetic force at plasma disruption are calculated for the FER. The induced voltage between adjacent modules is estimated as ~75 V in case of 24 blanket modules.

The electromagnetic forces at disruptions are calculated for two kinds of the plasma current decay scenarios, i.e. 1) exponential current decay, 2) liner current decay. In the latter case, the maximum

electromagnetic force is one and a half times as large as that in the former case. Since the supports of modules would not be rigid because of the restriction on accessibility behind the inboard blanket modules, they would not withstand the induced forces when the conductive shells are installed in them.

In addition to the results mentioned above, the chapter 5 describes the vertical stabilty experiment on Doublet III, and data bases of the JT-60 plasma control system, the JFT-2M equilibrium control system and fast pulse power supply technology, and irradiation effects on coil insulation materials and shell materials.

The results of the benchmark calculations specified in INTOR workshop are also provided for stabilization simulations of plasma vertical position, and eddy currents and forces at plasma disruption. Three configurations of passive elements are analized for vertical position control. One filament model is used for the plasma in these models, and a distributed current model is also used in the simplest one of these passive models. The disruption analysis is carried out for only one passive model.

Table 3.1 Summary of sensitivity studies on stabilizing properties of high conductive shell structures.

MODEL NO.	NO. OF DIVISION	INBOARD		OUTBOARD			GROWTH TIME: τ_G (ms)
		F/W	S/W	F/W	S/W	E/W	
10	14	SS (10)	SS (20)	Pb (60)	Cu (15)	NONE	32.21
20		Pb (60)	Cu (15)				41.04
30	28	SS (10)	SS (20)				17.74
31				Pb (100)			20.62
32				Pb (60)	Cu (22.5)		21.90
33				Pb (100)			26.29
40		Pb (60)	Cu (15)	Pb (60)	Cu (15)		27.62
50		SS (10)	SS (20)			Cu (15)	19.73
80	42	SS (10)	SS (20)			NONE	9.27
90		Pb (60)	Cu (15)				17.07

F/W: FRONT WALL S/W: SIDE WALL E/W: END WALL

FIGURES IN ( ) IS THICKNESS; mm

Table 3.2 Parametric studies on plasma position control.

			MAX. VOLT (V)	MAX. CURRENT (kA)	P/S CAPACITY (MVA)	MAX. DISPLACEMENT (mm)
$V_L = 8$	Z_{gnt} (mm)	0.0	612	118.5	72.57	−18.27
		2.0	630	118.5	74.67	−18.24
		5.0	700	120.7	84.50	−18.32
	τ_{Bd} (msec)	1.0	612	118.5	72.57	−18.27
		2.5	534	117.1	62.50	−15.59
		5.0	438	112.5	49.21	−12.64
	T_{delay} (msec)	0.5	615	115.2	70.87	−17.83
		1.0	612	118.5	72.57	−18.27
		2.0	592	125.9	74.49	−18.92
	T_{dead} (msec)	0.5	588	115.3	67.80	−17.62
		1.0	612	118.5	72.57	−18.27
		2.0	661	126.5	83.69	−19.56
$V_L = 250$ V	Z_{gnt} (mm)	0.0	250	132.4	33.09	−19.08
		2.0	250	132.0	33.01	−19.05
		5.0	250	133.1	33.28	−19.17
	τ_{Bd} (msec)	1.0	250	132.4	33.09	−19.08
		2.5	250	128.3	32.08	−17.47
		5.0	250	121.4	30.35	−14.62
	T_{delay} (msec)	0.5	250	130.4	32.60	−18.90
		1.0	250	132.4	33.09	−19.08
		2.0	250	135.8	33.95	−19.35
	T_{dead} (msec)	0.5	250	129.2	32.30	−18.66
		1.0	250	132.4	33.09	−19.08
		2.0	250	138.6	34.66	−19.90

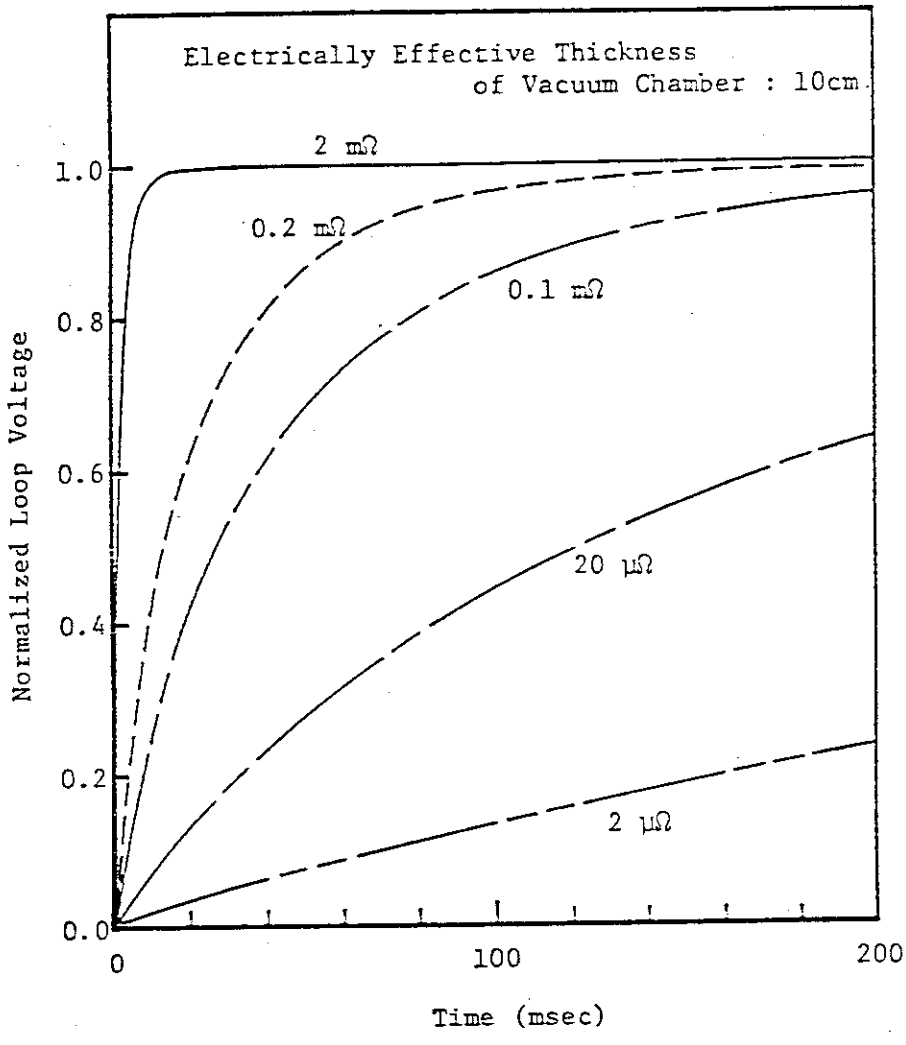

Fig. 3.1 Time evolution of normalized plasma loop voltage as a function of bellows resistance.

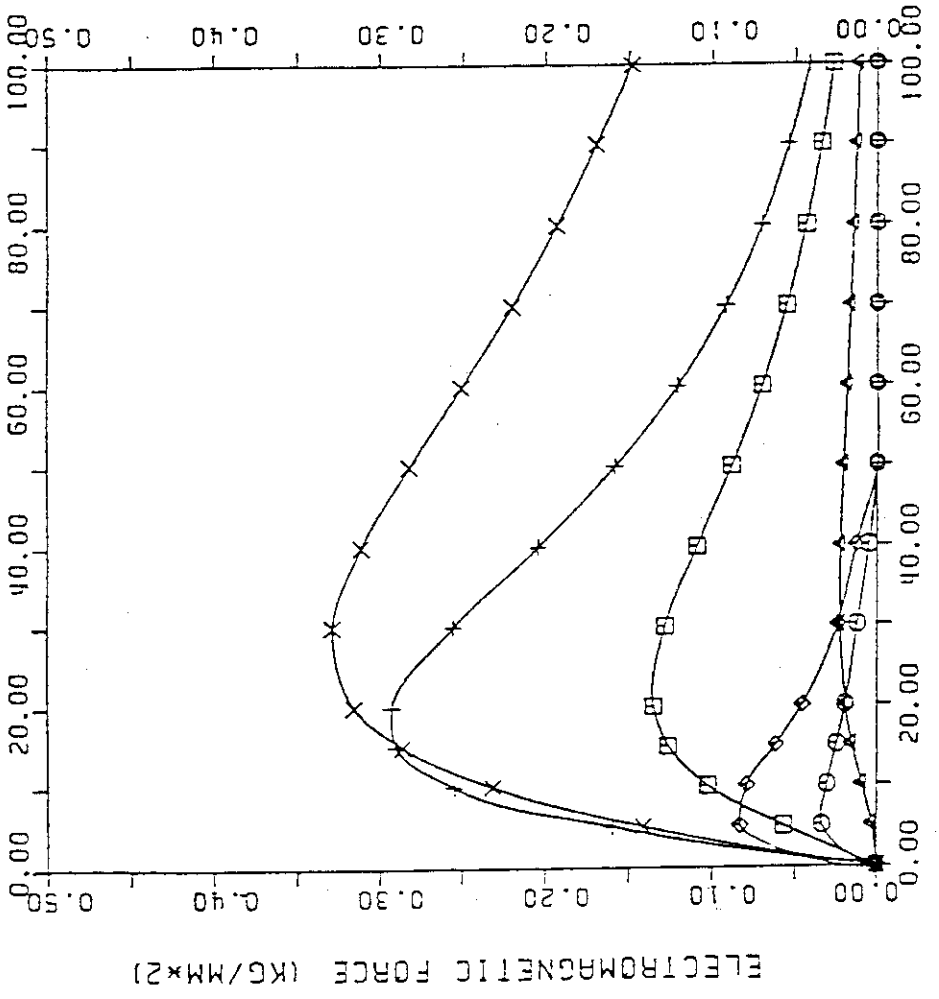

Fig. 3.2 Time dependence of electromagnetic forces due to toroidal magnetic field during plasma disruption. Plasma current decays exponentially with a time constant of 15 msec.

4. Maintainability

In the personnel access reactor concept which were developed in INTOR Phase 0, Phase I and Phase IIa Part 1, maintenance operations external to the reactor are expected to be accomplished in a hands-on mode. And all internal operation such as replacement of divertor or blanket should be remotely accomplished.

On the other hand, in the all-remote reactor concept which excludes the personnel access to the reactors, all operations should be carried out remotely and there is no requirement in order to permit personnel access. In the case of all-remote reactor concept, as there is no personnel access to the reactor from the view point of maintenance, biological shield is not necessary and baking of the vacuum chamber in order to evacuate the tritium seems to be unnecessary, and immediate access to the reactor by remote machine is possible just after coil shutdown without waiting the decay of induced radio-activity of the reactor structure.

The purpose of the study is to examine the impact of all-remote access concept to the reactor system and to establish a comparison with that of personnel access concept.

The goal of the study is to estimate the relative cost and the impact on repair and maintenance system.

The following items are considered in order to compare both design concepts.

① Reactor structure dimension, ② TF/PF coils, ③ Dose rates/ shield requirement, ④ Tritium containment and control, ⑤ Maintenance procedure/maintenance device, ⑥ Reactor building, ⑦ Capital and operational costs.

(1) Tritium containment

During reactor operation, the tritium containment is performed by vacuum enclosure (plasma vacuum chamber) and reactor building. During maintenance such as replacement of divertor or blanket, as the vacuum enclosure is opened, the tritium containment is performed by reactor building. The tritium containment concept is same both for personnel access concept and for all-remote concept.

(2) Tritium cleanup criteria

According to the ionization radiation hazard protection rule in Japan, the allowable tritium concentration level is $<5\times10^{-6}$ Ci/m^3. During maintenance operations such as retraction or insertion of internal reactor component, there is tritium release from first wall into the reactor room. For personnel access, the tritium concentration level in reactor room should be lower than 5×10^{-6} Ci/m^3.

Two cases of tritium release and its treatments are considered.

① When vacuum enclosure is opened without baking after reactor shut down, the tritium release rate from the first wall is $\sim 10^2$ Ci/day.

Tritium release will continue a month (maintenance time), then total tritium release in the reactor room is $\sim 3\times 10^3$ Ci. This amount of tritium should be recovered by a large recovery system to avoid the excessive soaking effect even though any personnel access is not considered.

The emergency tritium cleanup system with 1.5 m^3/sec. permits the tritium concentration level in the reactor room to reduce to the range $<5\times 10^{-6}$ Ci/m^3 with the delay of one week after the maintenance completed. For all-remote concept, the vacuum chamber bake out for detritiation is not required but desirable.

② When vacuum enclosure is opened with baking (150°C, during a week) after reactor shut down, the tritium release rate from the first wall is ~ 2 Ci/day.

In order to sustain the tritium concentration level in the ranges 5×10^{-6} Ci/m^3, the process flow rate (>4 m^3/S) is required. This will be possible by a large ventilation system as far as the total amount of tritium will not exceed the waste limit.

(3) Shielding requirement

The following conditions are considered as basis of the design.

① Dose rate at the outside of shield: 2.5 mrem/h. for personnel access concept.
(for all-remote concept, only the protection of TF coil is considered.)

② Dose rate at the outside of reactor building wall for both personnel access and all-remote concepts: 0.1 mrem/h.

With above conditions, the thickness of outer shield and reactor building wall for personnel access and all-remote concept is estimated. Nuclear heating in TF coil for both concepts is also estimated as follows.

	Personnel access	All-remote
Thickness of the reactor building wall	1.5 m * (2 m)**	2.6 m
Thickness of the outer shield	1.05 m	0.55 m
TF coil nuclear heating	3 kW	8.6 kW

* Requirement from shielding
** Requirement from building structure

(4) Configuration parameters

For all-remote concept, the elimination of the biological shield permits the reactor to be more compact by virture of the reduction of 50 cm in thickness of the outer shield structure.

As a result, the sizes of TF coil and PF coil are slightly reduced. The reactor concept for personnel access and all-remote are performed.

The main characteristics relative to TF/PF coils and the torus structure for both cases are as follows.

	Personnel access	All-remote
TF coil bore	6.6m × 9.3m	6.1m × 9.0m (ripple 1.8%)
AC loss of TF/PF coils	204.4 kW	158.1 kW
PF coil ampere turn	96 MAT	108 MAT
PF coil power supply (MG peak power)	2.3 GW	1.9 GW
Diameter of cryostat	24.5 m	23.5 m

(5) Maintenance requirements and scenario considered

In order to determine the delay for access to the reactor after reactor shut down for both concepts, several time intervals are taken into consideration.

The time intervals considered for access to reactor are as follows.

Items	Hours
TF coil shut down time	20 h
Dose rate to 2.5 mrem/hour	24 h
Heating to 150°C for baking	32 h
Baking time for personnel access	∿168 h (1 week)

For all-remote concept, as there is no human access, no baking nor reduction of dose rate is required. Therefore, only the delay of TF coil shut down time is sufficient for access of remote maintenance device. For personnel access concept, when only the access around the reactor such as inspection is required, the delay of 24 h. required for reduction of dose rate is sufficient. However, when the plasma vacuum chamber should be opened for the purpose of repair and maintenance of internal components, the baking is indispensable.

The delay time required for access to reactor are as follows.

Items	Hours
Personnel access for replacement	200 h
Personnel access for inspection	24 h
All-remote access { for replacement / for inspection }	20 h

Being taken into consideration the delay time for access, the comparison on repair and maintenance time between personnel access and all-remote concept is as follows.

Items	Personnel access concept	All-remote concept
Replacement time of blanket	30 days (single) 47 days (multiple)	19 days (single) 39 days (multiple)
Replacement time of divertor (limiter)	19 days (single) 37 days (multiple)	11 days (single) 31 days (multiple)

The difference of time for maintenance between personnel access and all-remote results mainly from the exclusion of baking evacuation for tritium removal in all-remote concept.

(6) Maintenance equipment requirements

All remote equipment must use sensor, actuators, etc. which are reliable under strong radiation. Materials which don't tend to be irradiated should be selected as structures. As for personnel access equipment, it isn't always necessary to consider the irradiation effect. But it is wise to do that, if we consider the serious accident such as LOCA.

However the function of the all-remote maintenance equipment basically is not very different from that of the personnel access one. Because all the remote maintenance equipment should be of simplicity of mechanism, high reliability, and high efficiency of work.

INTOR maintenance requires following remote maintenance equipments.

① overhead crane, ② access door carrier, ③ divertor extraction vehicle, ④ blanket extraction vehicle, ⑤ auto-seal cutter/welder, ⑥ auto pipe cutter/welder, ⑦ bolt runner, ⑧ floor-mobile manipulator, ⑨ overhead servo manipulator, ⑩ overhead power manipulator, ⑪ in-vessel inspection vehicle, ⑫ ex-vessel inspection vehicle, ⑬ work supervising system, ⑭ N.D.T. system, ⑮ jigs and tools, ⑯ vacuum leak detecting system.

(7) Costs

The typical cost fractions are determined following the conclusion of the cost and schedule group in the Phase IIA Part 1 workshop. Detailed cost fractions, for example "shield" contribution in "torus + divertor", are calculated using Japanese cost evaluation for the case 2 in the benchmark assessment study of that group. The relative cost changes are calculated using differences listed below.

Component	Typical Cost Fraction (%)	A/P*
TF Magnet	21.5	0.92
PF Magnet	9.2	0.99
Shield	3.6	0.80
Reactor Building	8.3	1.28
M.G. Power for PF Magnet	8.2	0.82

* A: All-Remote Maintenance Design

P: Personal Access Design

The unit cost of the reactor building is taken to be weight (or volume) dependent although it was taken to be area dependent in the Phase IIA Part 1 workshop. About 1% of the direct capital cost change is lead from the above list. The cost reduction due to a smaller reactor size in the case of all-remote maintenance design is almost canceled by the increase of reactor building cost.

If we employ the same way to evaluate operating cost as the one in the Part 1 workshop, it changes very little since maintenance and decommission costs were calculated to be proportional to the direct capital cost. However it is possible that we have a significant difference of decommission costs between the all-remote maintenance and personal access designs due to reactor building activation.

(8) Data base assessment of maintenance equipment and R&D required

The existing technical data bases of the remote operation in Japan were checked whether this data base could be applied to the remote maintenance concept of fusion reactor system. Result is that the fundamental base is exist but the existing technical data base can't be applied directly to the fusion reactor.

These existing data are mainly developed for use at LWR plants or fuel reprocessing facilities, etc. There are several differences between fusion reactor and the other nuclear facilities: condition of circumstance, characteristics of the object to be repaired, etc.

The demonstration of remote technologies to fusion maintenance problems is necessary and the continued improvements in robotics and electronic hardware and software are expected.

(9) General conclusions

In this study, we have re-examined the present personnel access reactor concept and developed an all-remote reactor concept which is oriented to reduction of reactor size. And we have compared both design concepts in focusing our attention to reactor structure size, TF/PF coil size, dose rate/shield requirement, tritium containment and control, maintenance device, reactor building and finally to capital and operational costs.
About 1% of the direct capital cost reduction is obtained.
Concerning the operating cost, it is possible that we have a significant difference of decommission costs between all-remote concept personnel access concept attributable to reactor wall activation.

The conclusion of this study is that a configuration based on all-remote operation concept with biological outboard shield which allows limited personnel access is the most effective design for maintenance.

5. Technical Benefit

Technical benefit of partioning INTOR component design and fabrication.

5.1 Purpose and Scope

The purpose of this critical issue is to examine the implication of having four participants fabricate components of a major system of INTOR. There are potential advantages and disadvantages from such an approach, and so a systematic examination of them will be performed.

Informations of an identification of differences between fabrication by a single manufacturer and fabrication by multiple manufacturers, would be most helpful in progressing the international joint project of the four INTOR participants.

5.2 Technical benefit

Technical benefit is defined as follows;

(1) Technical transfer of advanced technologies developed in INTOR project among four participants.

(2) Development of industrial capability and experience for furture fusion reactor technology.

5.3 Basic assumptions of technical benefit evaluations

(1) Reference organization scheme
A reference organization scheme is characteriged as shown in Fig.5.3-1 and its responsibilities are given also.

(2) Three scenarios for realizing INTOR
Three scenarios are shown in Table 5.3-1. Scenario A is the reference for comparison between international partitioning approaches, scenario B and scenario C, and a purely national approach, scenario A.

(3) Reference cost
International average figures as of phase II A Part 1. (Case 8)

(4) Reference schedule
Phase II A Part 1.

(5) Classification of systems/comp. in scenario B and C. Table 5.3-2.

(6) Approximately equal shares per participant.

5.4 Evaluation results

(1) The relative cost evaluation between three scenarios for total cost per participant is shown in Table 5.4.1.

(2) Schedule evaluations are based on the evaluations of incremental time in the questionaires and on the consideration of preserving the relation among preceding and succeeding items in the schedule. From INTOR design and construction schedules of scenario B & C, the net increase of total schedule is about 1.8 years in scenario B and about 1.0 years in scenario C.

(3) Evaluation of partioning on construction process in performed for impact of scenario B & C and the result shows that scenario C is superior to scenario B. This coresponds to results of cost evaluation, that is, the partioning of scenario B needs a lot of manpower and leads to cost-up of INTOR construction.

(4) From the answer of No. 15 in the questionnaires, scenario C is estimated to be risky. The risk needs to be emphasized that, in case of scenario C, there would be a great damage for INTOR project execution if a participant shoud fail in the fabrication of one component.

(5) Information exchanges for technical transfer are indispensable for scenario C, which only one participant is engaged in the fabrication of one component in advanced technology areas, but an effort has to be made for fruitfull information exchanges. On the otherhand, in case of scenario B, information exchanges will be made successfully on the same technology base, because four participants execute the same R&D and fabricate the same system.

5.5 Conclusion

The following conclusions were obtained that from benefit evaluations of cost, manpower and schedule, scenario C is superior to scenario B, and to the contrary in the technical informaion exchange and the risk, scenario B, is most promising. From the definition of technical benefit, scenario B seems to be very favorable for technical transfer of advanced technologies developed in INTOR project. In order to adopt scenario B, technological level of each participant is necessary to be almost equivalent at the start of INTOR construction and so, each participant should make a great effort to develope his own technology basis. On the other hand, the INTOR central team should be consisted of many staffs with strong management power and strong technology power, for the purpose of successful INTOR project in scenario B.

Fig. 5.3-1 Reference organization scheme

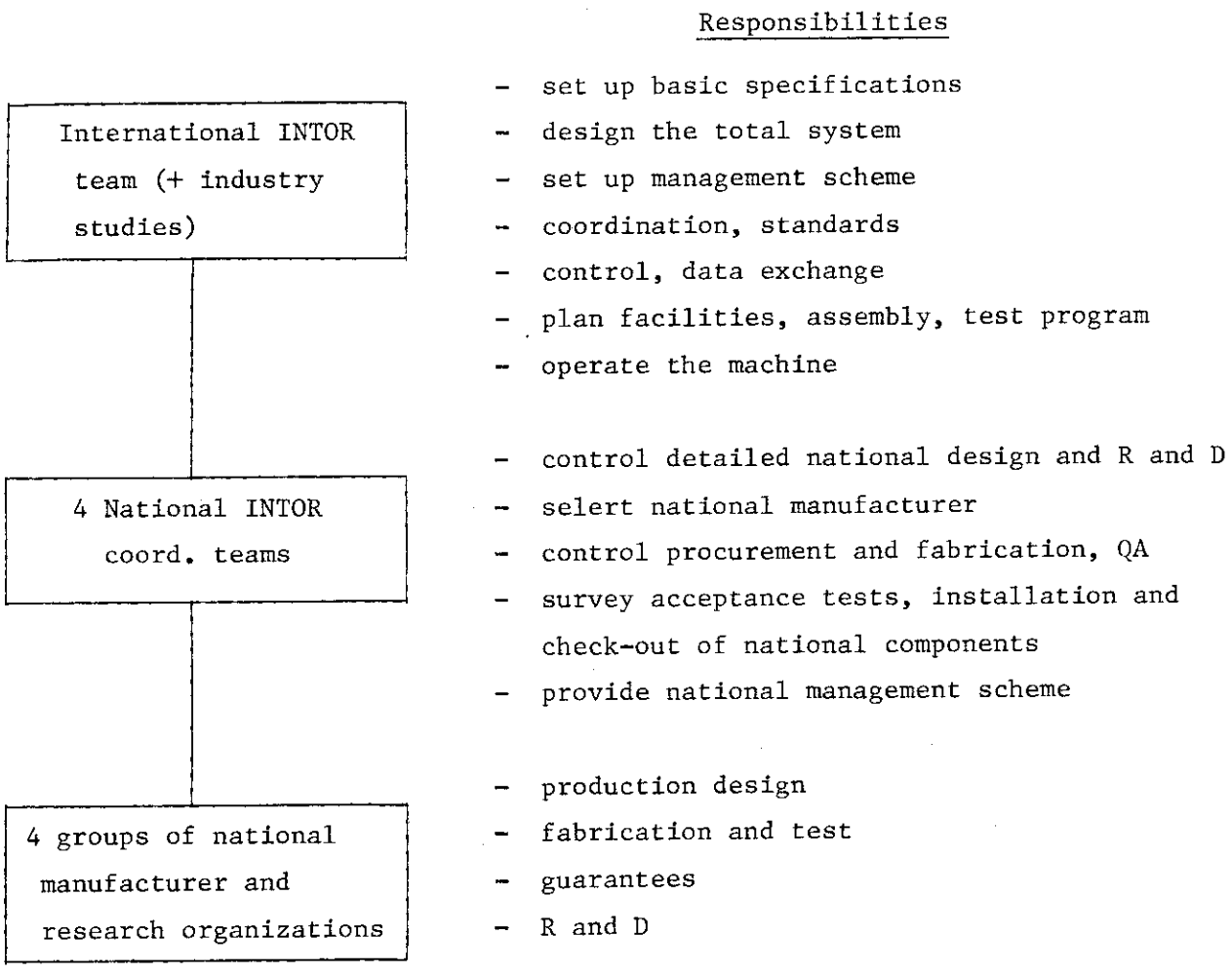

Table 5.3-1 Three Scenarios for realizing INTOR

A	B (advanced technology components split, conventional technology components branch)	C (branch)
Four nations each build their own "INTOR" based on their national R and D = reference case for benefit evaluation	One international machine is built by four nations based on four national R and D programs sharing fabrication of multiple high technology components and of the different conventional components.	One international machine is built by four nations based on four national R and D programs sharing fabrication of different components.

Table 5.3-2 Classification of systems/comp. in scenario B and scenario C

No.	Systems/comp.	scenario B		scenario C		Remarks
		Multi.	Diff.	Multi.	Diff.	
1	Reactor systems					Multi: multiple high technology components
	1 Torus					
	Divertor	○			○	
	Blanket sector	○			○	Diff: different conventional components.
	Blanket test module	○			○	
	Shield sector	○			○	
	First wall	○			○	
	Mechanical support		○		○	* in scenario C, all divertors are fabricated by one participant.
	Pumping system	○			○	
	2 Magnet					
	TF magnet	○			○	
	PF magnet (solenoid)	○			○	
	PF magnet (ring)	○			○	
	Cryostat	(○)	○		○	
	Mechanical support	(○)	○		○	
	Refrigerators		○		○	
	3 Heating					
	ECRH	○			○	
	ICRH	○			○	
2	Supporting systems					
	1 Fueling	(○)	○		○	
	2 Electr. supply					
	TF		○		○	
	PF		○		○	
	RF		○		○	
	3 Tritium		○		○	
	4 Cooling		○		○	
	5 Diagnostics		○		○	
	6 Maintenance		○		○	
3	Facilities		○		○	

Table 5.4-1 Relative cost per participant

Item	Scenario		
	A	B	C
Relative cost per participant	1.0	0.43	0.32

6. Physics

Stability limits

(Beata limits)

As for the experimental effort to attain a higher beta equilibrium, extensive studies on the low q_s discharges under the condition of a relatively low toroidal field were continued in Doublet III from the viewpoint that the higher beta value could be attained for the lower q_s discharge. In order to attain the very low-q stable discharge in the Doublet III ramping of the plasma current during the NBI heating is effective. By the technique the plasma with safety factor as low as 2 and 1.5 were obtain for the plasmas with large ($0.41 < a < 0.44$) and small ($0.34 < a < 0.38$) minor radii, respectively. In these experiments the maximum beta values are 3.3 % and 4.5 % in the respective order. An extensive effort to get higher plasma pressure, i.e., a high beta value at higher toroidal field strength has been also made. In the series of the experiments the volume average beta of about 2 % is obtained for the toroidal field of 2.2 T, where $T_e(0) \sim 5$ keV, $T_i(0) \sim 5.5$ keV, $n_e > 6.5 \times 10^{13}$ cm^{-3}, with 8 MW NBI heating.

At present quantitative discussion on the beta limit is possible only within the framework of the MHD stability analyses, sometimes with taking into account of modification by kinetic effects. We summarize the four topics on the stability analyses which relate to the beta limit of the tokamak plasma, i.e., the analyses of the infinite-n ballooning mode, the finite-n kink mode, the beta scaling law due to the modes, and the finite-n ballooning modes.

In general a growth rate of a higher-n mode is higher and infinite-n ballooning modes are considered to play the most crucial role on the limitation of the plasma pressure. These instabilities are sensitive to the shape of the plasma cross section, pressure anisotropy, pressure profile, and current profile. In order to obtain a high beta equilibrium stable against the infinite-n ballooning modes, optimization with respect to these parameters is required.

The dependence of the critical beta value on the safety factor at the plasma surface is studied in the wide range of the ellipticity and the triangularity of the plasma cross section. The safety factor at the magnetic axis q_0 is unity. The triangular deformation of the elliptic tokamak increases the critical beta value considerably, especially, in the low q_s region. By fits on the numerical results, Takizuka got the following formula of the critical beta value for $q_0=1$,

$$\beta_c(\%)=\frac{30\kappa^{1.5}}{Aq_s}\{1+0.9(\kappa-1)\delta-0.6\frac{\kappa^{0.75}}{q_s}+14(\kappa-1)(1.85-\kappa)\frac{\delta^{1.5}}{q_s^4}\}.$$

Figure 6.1 shows that numerically obtained critical beta values are well represented by the above formula. Elongation and triangular deformation cooperatively increase the critical beta value.

Another important result of the analysis is the dependence of the critical beta value on q_0. The critical beta value can be increased by increasing q_0. This improvement by large q_0 is also strongly related with the triangular deformation of the plasma cross section and the increase of q_0

reduces the critical beta value for a purely elliptic tokamak, as expected by the theoretical prediction.

In summary optimized high beta equilibrium stable against only the infinite-n ballooning mode is obtained by choosing simultaneously high elongation, high triangularity, high q_0, and low q_s. It is very important to investigate whether this kind of optimized equilibrium is accessible or not. Further studies are necessary on other kinds of instabilities by taking into account of the transport and/or heating processes. The result of the kinetic analyses shows that the transition between the stability and instability regions of the MHD modes is smooth and suggests the soft beta limit. But conclusion on the implication of the instability on the beta limit requires more extensive analyses of infinite- and finite-n modes including 3-dimensional nonlinear simulations.

Free boundary modes remain unstable for the optimized equilibria against infinite-n ballooning mode. By using the ERATO code Tsunematsu et al. studied the stability of the free boundary modes for the same equilibria as those for the infinite-n ballooning mode. The n=1 kink mode is the most unstable and the beta limit for $n>1$ is almost the same as that for the infinite-n ballooning mode. The formula for the critical beta against the n=1 kink mode is expressed similarly as in the case of the infinite-n ballooning mode as

$$\beta_c(\%)=\frac{C\kappa^{1.65}}{Aq_s}\{1+(\kappa-1)\delta\} \quad C=14\ (2<q_s<3)\ \text{and}\ C=20\ (3<q_s<4),$$
$$\beta_c\sim 0 \quad \text{for}\ q_s<2, \qquad (1.2.1.5)$$

where inverse proportionality on the aspect ratio is assumed.

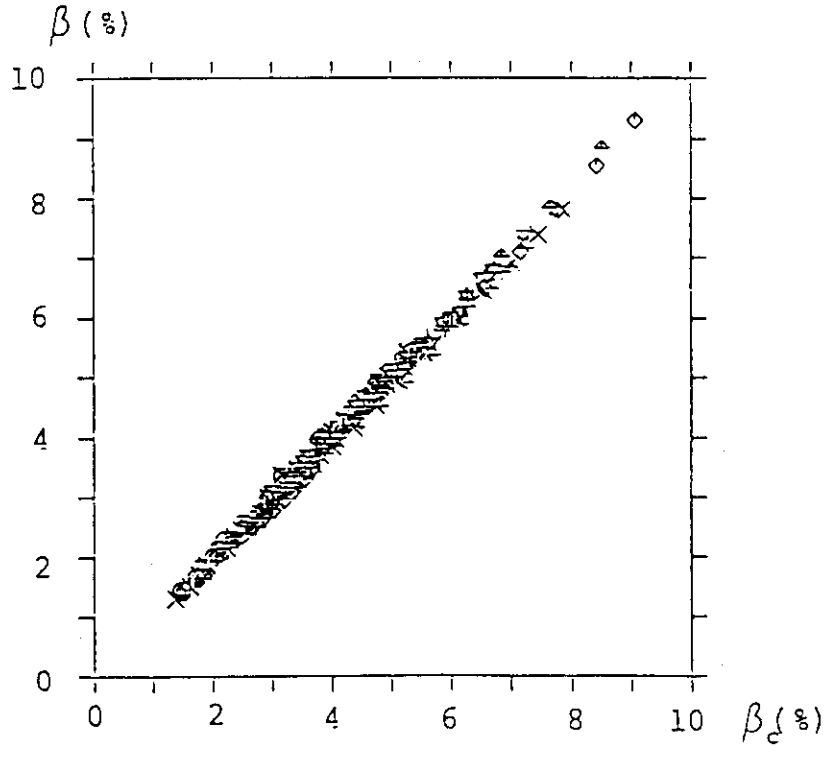

Fig. 6.1 Critical beta value for infinite-n ballooning mode. Numericalluy obtained beta β is well represented by β_c.

In deriving a more convenient expression it should be noted that the critical beta value is approximately proportional to the plasma current in a practical or conservative tokamak. This tendency is also observed in the case of the n=1 kink mode. And both of the equations for the ballooning and kink modes are roughly expressed in the range of q_s 2 by using the toroidal plasma current I_p as

$$\beta_B(\%) = (20 \pm 2.5)\mu_0 I_p / (2\pi a B_{t0}) \quad \text{for ballooning mode.} \qquad (1.2.1.6)$$

$$\beta_K(\%) = (16 \pm 2.0)\mu_0 I_p / (2\pi a B_{t0}) \quad \text{for } n=1 \text{ kink mode.} \qquad (1.2.1.7)$$

Systematic parameter survey of the finite-n ballooning modes still consumes a lot of CPU time and only typical cases are studied and qualitative results are obtained as for the feature of high beta equilibria of a tokamak plasma. As examples of the low-, middle-, high-n ballooning modes Tsunematsu et al. studied the n=3, 10, and 50 modes, especially, to find the second stability region and investigate the dependence of the stability of ballooning modes on pressure profiles. Optimization of the current profile remains effective for the stabilization of the middle- as well as low-n modes. Also it seems that the external kink mode will be a beta limiting instability after the optimization with respect to the finite-n ballooning modes is carried out.

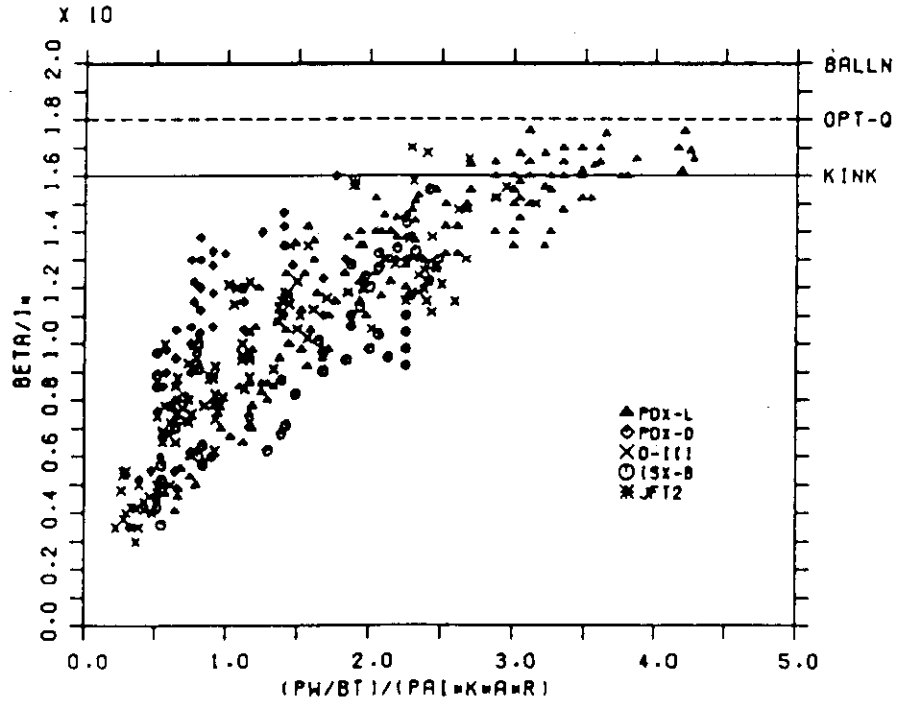

Fig. 6.2 Comparison of the experimental data and the theoretical predictions of the beta limit.

We obtained scaling laws which give the accessible beta value of tokamaks by the optimization of the pressure profile against infinite-n ballooning mode and by stability analyses of finite-n free boundary modes for the optimized equilibria. These scaling laws are roughly expressed as $\beta_c = CI_p$ for $q_s > 2$. This kind of parameter dependence is predicted by several theoretical groups in the world and the comparison between this theoretical prediction and experimental data obtained up to now is presented in Fig. 6.2. From this figure it seems rather difficult at present to attain a high beta state above the theoretically predicted limit. And it seems reasonable that the equation $\beta_c = CI_p$ gives a practical beta scaling law for a standard tokamak of the present day.

(Density limits)

Density limit of a tokamak is well represented by the DITE plots, where operational regimes with high density and low safety factor are clearly shown together with the advancement of the used experimental techniques. In Doublet III, JAERI team has carried out experiments on high density and low q discharges. Wall conditioning with TDC and Ti gettering and choice of TiC coated graphite as limiter material have resulted in the highest Murakami parameter of 10×10^{19} $m^{-2}T^{-1}$ with NBI heating.

Experiences obtained through these studies are as follows: (1) The Murakami scaling of density on B_t/R is effective to describe the operational regimes of a tokamak plasma the Murakami parameter well represents cleanliness of the plasma. Clean vacuum condition is one of necessary conditions to obtain a high density plasma, because the ratio of radiation loss rate to input power has some threshould value. In ohmic heating, it lies at 40-80 %. (2) In ohmic heating without Ti gettering, the Murakami parameter lies in $2\text{-}4 \times 10^{19}$ $m^{-2}T^{-1}$ and with Ti gettering in $4\text{-}8 \times 10^{19}$ $m^{-2}T^{-1}$. Additional heating increase the value up to $6\text{-}10 \times 10^{19}$ $m^{-2}T^{-1}$. The ratio of radiation loss to input power has a tendency to take a lower value in the case with additional heatings. (3) In order to obtain a high density and low q plasma, careful programming of the plasma current and gas puffing rate, and appropriate postion control are necessary. If it is not the case major disruption terminates the discharge.

(Disruptions)

We have not yet reached a comprehensive even phenomenological description of the disruption by which we could logically classify the variety of existing experiments. The important informations needed to understand and overcome the disruptions are: conditions of the disruptions, detailed description of the time evolution, frequency, heat deposition profiles, and density and current limitations. Experiments aiming at developing techniques to increase density and to lower q_s values are also closely relating topics. One of the very important questions concerning the mechanism of the major disruption is what kind of the MHD modes exist and whether the modes are external or internal ones.

A systematic study of the disruptions was carried out in DIVA. The results obtained in the series of the experiments are summarized as follows: (1) after reducing impurities no major disruption was observed, (2) by injection of neon gas at q_s=2.5, radiation loss increased and the disruption was excited, (3) m=2/m=1 precursor oscillation was observed before the

disruption and for the plasma with q less than 2 disruption did not appear. These results seem to confirm the disruption scenario of the nonlinear tearing mode origin. On the other hand the experiments carried out in JFT-2 tokamak suggested that the disruption is caused by the m=2 kink mode.

The first series of JIPP T-II experiments insisted that the observed disruptions are classified into three types: (1) soft major disruption caused by the overlapping of the m=2/n=1 and m=3/m=2 magnetic islands, (2) soft major disruption caused by direct contact of the m=2/n=1 magnetic isoland to the limiter, in which the m=3/n=2 magnetic island plays no role in the disruption process, and (3) hard major disruption which is caused by a simultaneous contact of the m=2/n=1 island with both the m=3/n=2 island and the limiter. The second series of the disruption experiments concluded that an m=1/n=1 mode coupled with dominant m=2/n=1 mode is responsible for the major disruption. The disruption scenario is rather sophisticated and roughly summarized as follows; (1) establishment of broad current profile by accumulation of impurites, (2) growth of an m=2/n=1 mode, (3) nonlinear growth of an m=3/n=2 mode, (4) occurence of a minor disruption, (5) establishment of narrow current profile, (6) growth of an m=1/n=1 mode, (7) establishment of flat current profile, (8) growth of an m=2/n=1 mode, (9) phase locking of the m=2/n=1 and m=1/n=1 modes, (10) asymmetric reconnection of the m=2/n=1 island, (11) occurence of a mjaor disruption.

Experiments by putting emphasis on understanding the disruption phenomena were also carried out in Doublet III. For the ohmic heating plasma very low-q discharge with q less than 2 has not been realized because of the disruptions. In the NBI heating experiments very low-q discharges with q_a as low as 1.5 have been realized. In the experiment two cases with and without the NBI heating at the current ramping phase were carried out and compared each other in order to investigate the effect of current ramping on the disruptions. The reason why the disruption is suppressed during the current ramping phase with the NBI heating is not clearly understood but it may be attributed to the change of the current and temperature profiles during the NBI heating.

There are several theoretical models to reproduce the experimentally observed major disruptions. Among them the models based on the nonlinear treating modes and the nonlinear kink mode are investigated minutely by numerical simulation codes. The former model relates the major disruptions in a plasma with profiles formed by edge cooling and the latter relates those in a plasma with the safety factor less than 2. As for the nonlinear tearing mode evolution model several different cases were numerically analyzed. Typical one of them is the disruption scenario of nonlinear destabilization due to the overlapping islands with m=2/n=1 and m=3/n=2 modes. This scenario seems very plausible because the typical phenomena of the major disruption, i.e., the negative voltage spike, decrease of the plasma temperature and extinction of the equilibrium due to the destruction of the magnetic surfaces can be explained successfully by the simulation on an edge-cooled plasma.

Confinement

Energy confinement properties of Ohmically heated plasmas in Doublet III were compared for D-shaped and circular cross section plasmas with an identical minor radius as functions of plasma current, electron density, and vertical elongation under a wide range of discharge conditions. It indicates that the electron energy confinement time is proportional to the product of the average density and the safety factor with an elongation effect.

In the low density regime, the gross energy confinement times of Ohmically heated plasma in DIVA, JFT-2, Doublet III, JFT-2M and JIPP-T II are almost same as that expected by neo-Alcator scaling ($0.19\times10^{-20}\bar{n}R^2a$). In gas fueled diverted Ohmic discharges, the recycling and the neutral pressure both at the edge and the divertor region, increase nonlinearly as the density is raised above 4×10^{13} cm^{-3}. The energy confinement time saturates near 60 ms. In contrast to that, the pellet fueled confinement times continue to improve with increased density. This is probably due to the fact that in the pellet fueled discharges both the edge pressure and the limiter recycling are maintained at relatively low levels and/or the successful density rise at the plasma center which leads to good confinement properties.

The neutral-beam heating experiments in Doublet III, JFT-2, and JFT-2M showed degradation (L-mode) of confinement in comparison to the Ohmic heating case. Recently, H-mode discharges have also been observed in divertor operation in Doublet III. The observation of the recycling particle flux intensity at the main plasma edge for various limiter and divertor discharges indicates that the gross energy confinement of beam-heated discharges is closely related to the intensity of the edge particle flux. The divertor equilibria allow a wide variety of edge recycling, depending on gas puff intensity, rotational transform of scrape-off field line, plasma current, etc. Divertor discharges with low particle recycling around the main plasma show better energy confinement than limiter discharges at high plasma densities. The energy confinement time of these discharges is proportional to n_e (Fig. 6.3). The improvement in the confinement time may stem primarily from the reduction of heat transport in the main plasma edge region, which is associated with the reduction of the recycling particle flux at the main plasma edge.

Recent Doublet III experimental results with high plasma current (1 MA) and high power (8 MW) NBI heating with hydrogen and deuterium beam indicate that the central ion and electron temperature of H-mode discharge increase almost linearly to the absorbed power up to 7MW and attains more than 5 keV (Fig. 6.4). The amount of energy stored in the plasma measured by the diamagnetic loop increases almost linearly with the increase of absorbed power. The volume averaged beam component of high NB heating is estimated to be 10-20 % (at $\bar{n}_e=7\text{-}4\times10^{13}$ cm^{-3}). The stored energy of a limitered discharges is still on the scaling $W_{st}=c(0.5+0.4P_{abs})$.

The improvement of energy and particle confinement in pellet produced plasmas has been established in both ohmic and beam-heated limiter and divertor discharges. The energy confinement is seen to improve with increasing density, in contrast to the saturation found in gas fueled plasmas. While the confinement of pellet-produced beam heated plasmas deteriorates with time and with increasing beam power, a method of interrupting the beams has produced sustained high confinement discharges with suppressing pellet edge

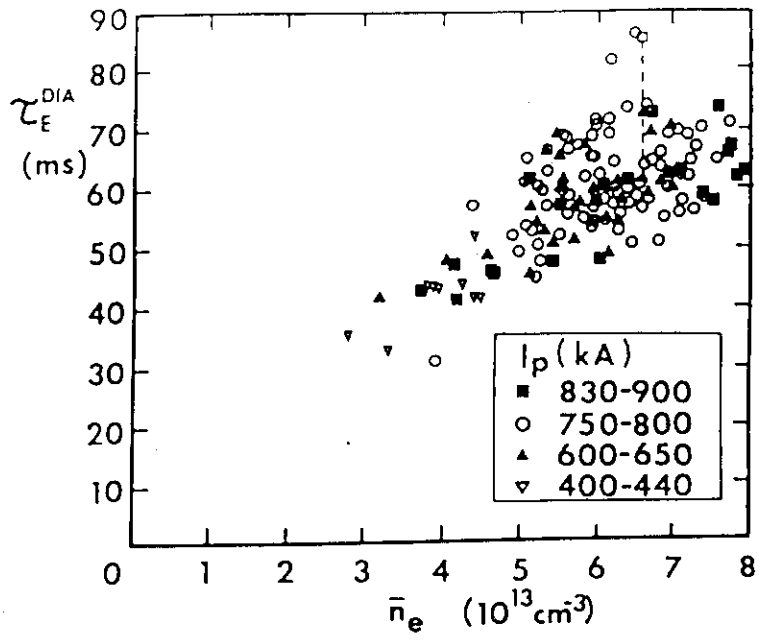

Fig. 6.3 Global energy confinement time. The confinement time of good divertor discharges increases as plasma density increases. B_T=2.0-2.6 T, hydrogen beam injection into diverted deuterium plasma. The energy confinement time during β_p increase is shown by for one case.

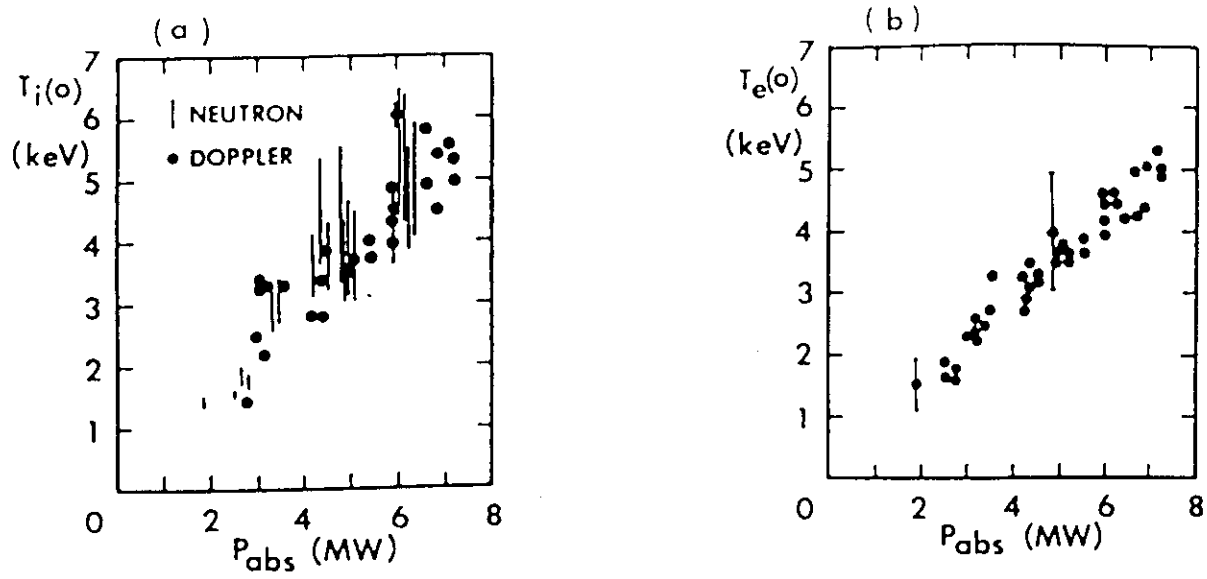

Fig. 6.4 Central ion temperature (a) and electron temperature (b) vs. absorbed power. The ion temperature by neutron has an ambiguity due to uncertainty of hydrogen (beam species) population. The electron temperature at $T_e > 4.5$ keV is measured by the grating 2 ω_{ce} radiometer. $\bar{n}_e$=4-7.5x10^{13} cm^{-3}, I_p=750-800 kA. B_T=2.0-2.6 T.

ablation. The enhancement of the ablation at the edge by neutral beam is found to be responsible for the confinement deterioration. A simple model calculation shows that the lower energy components of the beam particles which are supposed to deposit at the edge may be important for the edge ablation. The reduction of edge density and recycling seems to be a key aspect of the improved confinement along with the peaked central densities.

High power ICRF heating experiments have been performed in two ion hybrid heating regime in JFT-2M. The gross energy confinement time has an almost linear dependence on the line averaged electron density when the electron density is lower than 3×10^{13} cm^{-3}. The degradation of the gross energy confinement time in the ICRF heating is not so large as in the NBI heating case. We can not conclude that the slight deterioration of the energy transport or the radiation cooling by the impurities causes the degradation of the confinement time. The ICRF heated discharges in JIPP-T IIU also show that the gross energy confinement time increases with the density, and approaches to the value expected from the Ohmic scaling.

The Doublet III experiments show that the particle confinement time depends on the density and the plasma current in limiter discharges. The measurements show that the particle confinement time decreases with beam injection: 18-24 msec (Ohmic) to 7-18 msec (NBI). This means that edge particle recycling is enhanced with beam injection by a factor of 1.4-2.8 with respect to the ohmic heating level. The important feature is that the particle confinement time is proportional to the plasma current for beam-heated plasmas.

In JFT-2 the particle confinement time and the trapping efficiency were measured in various conditions. The results of particle confinement measurments show that, with injection, the particle confinement time levels off slightly as compared with the Ohmic heating case. The maximum reduction of the confinement time during the injection is 20 to 30 %. No appreciable difference was found between co- and counter-injection as far as the reduction of the particle confinement time is concerned, although no many cases were taken with counter-injection.

The toroidal rotation speed was measured in a series of Doublet III discharges by a spectrometer with wavelength shift of OVIII lines on a NBI beam path. For a constant value of plasma density and heating power, the peak rotation speed. The rotation speed is consistent with the toroidal phase velocity of the B_p fluctuation. Discharges with good confinement have a large rotation velocity, suggesting a close relationship between energy confinement and momentum confinement.

Neutral Beam Heating and Current Drive

JFT-2 was shut down in June 1982 after 10 years operation. A 2-MW neutral-beam injection (NBI) system and a 1-MW ion cyclotron range of frequency (ICRF) system were installed on JFT-2. The injectors are run in H_2. The NBI system consists of a co- and a counter-injector with an injection angle of 36° with respect to the plasma axis. Each beam line provides an ion beam of 65 A at 40 kV and species mix is 60 % H_1^+, 30 % H_2^+ and 10 % H_3^+. In the case of the two beams, 1MW co-beam and 1 MW counter-beam, the increment of poloidal beta is obserbed additive. The toroidal plasma rotation induced by the momentum input associated with NBI is unimportant in transport processes.

No rapid impurity accumulation occurs during counter-injection. Sawtooth oscillations change into the continuous mode when the poloidal beta value exceeds a critical value

In the JFT-2 tokamak, significant plasma heating is observed with simultaneous NBI and ICRF heating. With a net power of 2.2 MW (1.7 MW NBI and 0.5 MW ICRF) into D^+ plasma at a plasma density of 6×10^{13} cm^{-3}, the central ion temperature increases from 0.4 to 1.4 keV. In the JFT-2M tokamak, simultaneous heating of NBI and ICRF has been also performed. A theoretical analysis of ICRF wave heating in a plasma with neutral-beam injection (NBI) is performed. Wave propagation and absorption are examined kinetically in the presence of a high-energy ion beam component. The following findings are reported: 1) the wave coupling efficiency does not deteriorate by the beam; 2) co-operative heating is to be expected, and 3) selective heating of high-energy ions is possible.

The NBI system of JFT-2M consists of a co- and a counter-injection with an injection angle of 38° with respect to the plasma axis. Each injector is capable of delivering 1.2 MW to the plasma for 200 ms at a source voltage E_b of 40 kV and species mix is 72 % H_1^+, 22 % H_2^+ and 6 % H_3^+.

In the JFT-2M tokamak, a neutral-beam-injection (NBI) method to modify the distribution function f(v) in a velocity space of injected beam particles in a tokamak plasma has been developed. The method, multiple-short-pulse method, is characterized by the repetition period and the pulse length, and is expected to be a useful tool for the detailed investigation of slowing down process of injected beam particles and of NBI effects on plasma confinement. We have excited waves with this method in the ion-cyclotron range of frequencies (ICRF) due to beam-plasma interactions by an controllable manner. The theoretical analysis has shown that the high energy beam particles can excite the Alfven wave eigenmodes in the ICRF if the beam density exceeds a threshold and that the excited wave may contribute to the nonclassical energy transfer from the beam particles to the bulk plasma particles. It is very important to clarify the role of the excited wave on power balance in tokamak plasmas and the effects on plasma confinement.

The NBI system of DIII is designated to provide substantial auxiliary heating to a high density non-circular cross-section plasma. Near-perpendicular injection at approximately 27° to a radius vector at the plasma centerline, together with high energy hydrogen beams, is used to ensure substantial heating of the plasma core. Each ion source, when operating at a nominal 80 kV extraction voltage, delivers a beam whose approximate species mix is 60 % H_1^+, 30 % H_2^+ and 10 % H_3^+ to a close-coupled neutralizer. In DIII, energy confinement of beam-heated divertor and limiter discharges has been studied.

For the understanding of NBI heating experiments, both theoretical and numerical (Monte-Carlo) codes to calculate neutral beam trapping and penetration have been developed. The time dependent power deposition profiles are derived by using simple description of the local beam power fractions. Detailed non-time dependent beam power deposition is derived by an orbit following Monte-Carlo code. A new code which is time-dependent orbit following Monte-Carlo code is in progress. Another kind of orbit following Monte-Carlo code to derive the spectrum of charge exchange neutrals which enter into a diagnostic port has been developed to analyze diagnostic results.

There is no investigation of tokamak current drive using neutral beams in Japan. Only in Heliotron E, the experiment of neutral beam current was done. Induced toroidal plasma current flows in the same direction as neutral beam. Component of beam induced plasma current is 1.1 kA under neutral beam injection of 1 MW (28° injection, P_{abs}=0.5 MW) and observed toroidal plasma current should be composed of two origins, beam induced "Ohkawa" current and the diffusion-driven neoclassical "bootstrap" current. A current drive scheme based on combining neutral beam-injection and ICRF heating is investigated theoretically. The neutral beam injection mainly supplied toroidal momentum and is sustained by ICRF wave heating. The current is generated with sufficient efficiency and can sustain the tokamak plasma in a steady state.

Operation scenario

Detailed operation scenario of INTOR seems difficult now to be credibly specified from experimental experiences on JFT-2, JFT-2M, and Doublet III. Furthermore credible informations will be taken from the large tokamaks such as JT-60.

On JFT-2 and JFT-2M, the chamber wall and limiter are cleaned with TDC and gettering with titanium. To obtain a stable and clean plasma, the vacuum condition is a key factor. On INTOR, the measure of vacuum conditions must be also necessary and it must be solved that what method is applicable for vacuum conditioning, what measurement is appropriate and how to decide the critical value.

In the breakdown phase of JFT-2, pre-ionization with ECRH decreased the breakdown voltage to about half value of that without ECRH. The calculated inductive part of loop voltage agreed well to the measured one. So with a sufficient pre-ionization such as ECRH, plasma current may be built up easily with comparatively low loop voltage corresponding to the inductive part. After the breakdown, plasma current is planned to be raised with a rate of 1 MA/sec. This rate is not so high in comparison with results in JFT-2M and D-III. Before plasma current reaches near q=3, severe mhd instabilities may not appear. But near q=3, kink instability of m/n=3/1 and dangerous tearing mode of m/n=2/1 will be excited. Here, careful control of plasma parameters to overcome this barrier may be required, such as plasma density, plasma position and so on. In JFT-2M, initial current is raised with the rate of 1 MA/sec up to q=3.5, then plasma density is ramped up enough under nearly constant plasma current. Then rising rate of about 0.5 MA/sec is now necessary to run through the q=3 barrier. Key factors to overcome the barrier seems to be comparatively high density, clean plasma and moderate current rising rate. The barrier of q=2 is too hard to overcome.

As far as control of the plasma vertical control is concerned, in D-III, capability of non-circular plasma to obtain a high beta plasma has been demonstrated and elongation of 1.8 was achieved. On JFT-2M, elongation of 1.5 was also accomplished. But capability of vertical position control depends on the passive stabilization effects of vacuum chamber, poloidal coils and so on. Therefore it depends on the passive stabilization effects of inner compositions in INTOR that whether a stable divertor plasma with elongation of 1.6 can be obtained or not.

For control of plasma shape, in the initial build-up phase, nearly circular plasma may be a safety choice, and a desired plasma shape can be

established easily by modification from the circular plasmas. On JFT-2M and D-III, this method is used to control the plasma shape from a circular plasma to a D-shape plasma or to a divertor plasma.

As a main heating method, ICRF heating and NBI heating have been developed and a high beta plasma was demonstrated with NBI heating. In heating control, not only input power control but control of a high beta plasma are required. Control of a high beta plasma with good reproducibility is not yet established and experiments to get higher beta plasma is under way. Control techniques on current profile or pressure profile must be developed.

Burning plasma

The loss of alphas is mainly due to the ripple of toroidal magnetic field. This ripple loss was studied in detail by means of an orbit-following Monte-Carlo code. Collisionless ripple loss processes of suprathermal alpha particles are numerically investigated and the results agree fairly well with the theoretical prediction. The ripple-enhanced banana drift dominates the loss process of alphas. The ripple-enhanced power loss for the muximum ripple of 1 % is about 10 % of the total fusion power of charged particles. The effect of ripple on particle loss is also important not only for energetic but also for slowed-down alphas. The fraction of particle loss is about 1.5 to 1.8 times as large as that of power loss. The wall heat load due to loss alpha particles is localized, and its peak value reaches the order of 1 MW/m^2 if the muximum ripple exceeds 1 %.

Alpha-driven Alfven modes may cause an anomalous energy transport from alphas to bulk ions. The velocity inversion of alpha distribution, however, does not appear in an INTOR-like reactor. Perturbations of magnetic fields and electric fields due to ballooning mode instabilities can enhance the radial loss of alpha particles. ICRF waves in the additional heating phase can also affect the alpha confinement and thermalization. It is required to clarify these anomalous transports.

One of the practical proposals for burn control is active feedback control method performed by the plasma compression-decompression varing the vertical magnetic field. Recently, Ohnishi et al. carried out a one-dimensional plasma model to analyze the active feedback control by the plasma compression-decompression. It is shown that the thermal runaway can be suppress by the compression-decompression feedback control. The relative deviation of the major radius is within 1.2 %, that means the major radius moves 6.24 cm for INTOR case. Outward and inward shifts of the plasma major radius will compel the scrape-off layer increase for protecting the plasma in contact with a limiter on the midplane. Futhermore, this type of active control will require very accurate informations about the plasma state such as density, temperature and position. Although there are another possibilities for controlling thermal runaway, much works have to be done before the preferred method will be recommended. The passive control due to the beta limit oscillation is particullary atractive because the power production is a weak dependence on the ignition condition. Further progress in this area is expected.

7. Engineering

The Japanese contribution for Group G includes "Data Base Assessment", and studies on seven new tasks.

The Japanese current data base has been compiled mainly focusing on the superconducting magnet development and JT-60 project at JAERI.

The data base for magnet system has greatly advanced since the Phase 0 data base assessment through the LCT and CTP (Cluster Test Program) projects and the TMC-I (Test Module Coil) experiments. R & D requirements for the INTOR design data base are identified.

Satisfactory test results of the JT-60 NBI prototype have also demonstrated a great advance particulary in energy, power, and pulse length since the Phase Zero data base assessment. Problematic areas in R&D requirements for the INTOR-NBI systems are being reduced.

Systems engineering

A FOTRAN code "TORSAC" has been developed to evaluate a design concept and to make a sensitivity analysis. The code is now being upgraded with a main effort being paid on deciding PF coil locations automatically in accordance with plasma parameters.

Magnet systems

Results of current data base assessment and R & D requirements on magnet structures are summarized in Table 1.

A reasonable data base exists on mechanical characteristics of austenitic stainless steels, but generation of data on weld preparations is required.

Reliability of quality control techniques should be improved.

More informations are needed on radiation effects.

An extensive data base exists on the critical current characteristics of NbTi and Nb_3Sn conductors in strand size, but limited data is available on the effect of fatigue on critical current characteristics.

Little data exists on how much disturbance energy will be produced in an actual supersonducting magnet.

NBI systems

Results of JT-60 NBI prototype have almost satisfied the INTOR NBI requirements.

To increase overall power efficiency up to 50 %, it is necessary to develop direct recovery system with efficiencies higher than 80-90 %.

Table 1 Current Status of Data Base Assessment and R&D Requirements on Magnet Structures

		MATERIAL		TENSILE		FRACTURE		FATIGUE				RADIATION	
								S-N		da/dN			
				D.B.	R&D	D.B.	R&D	D.B.	R&D	D.B.	R&D	D.B.	R&D
METALIC STRUCTURAL MATERIAL		300SS Ser. NBS JAERI	BASE	○	×	○	×	△	○	△	○	△	○
			WELD	× △	○	× △	○	×	○	× △	○	×	○
		New SS HMSS JAERI	BASE	○	×	△	△	×	○	×	○	×	○
			WELD	×	○	×	○	×	○	×	○	×	○
	ICCS SHEATH	Incoloy 900 LLNL MIT	BASE	△	△	△	△	×	○	×	○	×	○
			WELD	×	○	×	○	×	○	×	○	×	○
		New SS HMSS JAERI	BASE	△	○	×	○	×	○	×	○	×	○
			WELD	×	○	×	○	×	○	×	○	×	○
ORGANIC MATERIAL		G-10CR,11CR FRP NBS		△	△	×	○	△	○	×	×	△	○

	○	△	×
D.B.(Data Base)	Adequet	Some	Few/None
R&D Requirement	Much	Some	Little

8. Nuclear

Data base of the nuclear technology for INTOR is assessed focusing on the following four fields ; Blanket, Shield, Tritium and Safety. Ongoing R & D programs in the above fields are also reviewed and required new programs are discussed.

(1) Blanket

Nuclear data file called JENDLE-3PR1 has been developed. This file includes newly evaluated nuclear data for ^{6}Li, ^{7}Li, ^{9}Be, ^{12}C, ^{16}O, Cr, Fe and Ni, and is used mainly for the analysis of the fusion neutronics experiments. In order to be used for fusion reactor design calculation the data for wider range of isotopes should be incorporated.

A number of computer codes and nuclear group constant libraries have been developed for the neutronics design of fusion reactors and for the analysis of integral experiments. They included group constants processing code, neutron and gamma ray transport codes, induced activity calculation code system and neutron and gamma ray group constants file.

With the two major intense D-T neutron sources, Japan is very active in the field of R & D of fusion neutronics. In JAERI, integral blanket neutronics experiments have being carried out at Fusion Neutronics Source (FNS) facility in two areas by using Li_2O as a breeding material. One is the basic benchmark experiment where the system is of simple composition and geometry to make the comparison with calculations as straightforward as possible in examining nuclear data and/or neutron transport methods. The other is the design-oriented benchmark experiment where the system incorporates the configurational complexity in radial direction of blanket design; it is not the mockup of a particular blanket design but for providing data base on the factors affecting tritium breeding or energy deposition, and to examine the overall accuracy of the calculation in a composite system.

The research program at the OKTAVIAN (Osaka University) directs more basic areas of fusion neutronics. Its major ongoing activity is the systematic measurements of double-differential cross sections of various materials to be adopted in fusion reactors by using a time-of-flight method.

While the fundamental aspect of fusion blanket neutronics can be studied by using present point neutron sources or their grade-up, neutronics engineering test will need higher intensity ($\sim 10^{15}$ n/s) and 3- dimensional volume neutron source, and more realistic simulation of blankets for precise evaluation of tritium breeding ratio and nuclear heat generation.

Data base assessment for the tritium breeding material is conducted sharply focusing on the Li_2O solid breeder.

Ongoing R & D programmes can be listed with the following headlines:

1) Fabrication and characterization of Li_2O and other solid breeders
2) Mechanical and chemical properties of Li_2O
3) Compatibility test of Li_2O and structural material
4) Mass transfer test of Li_2O
5) In-Situ tritium release test of Li_2O and other solid breeders
6) Radiation damge study
7) Irradiation integrity test of Li_2O and other solid breeders

The above programmes are addressing issues that need resolution in order to establish the viability of Li_2O solid breeder materials for blanket designs.

The compatibility data between Ni- or Fe-base alloy and Li_2O have been obtained. However the corrosion rate is strongly affected by the impurities such as H_2O or LiOH. Hence, it is necessary to measure the corrosion rate under the INTOR conditions.

For various experiments on Li_2O breeder, techniques has been developed to control impurities and to fabricate cylindrical Li_2O pellets by sintering. Discrepancy of porosity distribution properties will be attributable to the differences of measurement, fabrication process and starting material. Further experimental studies are desirable including microstructure control of Li_2O sintered pellet.

The data on tritium recovery are essential for the evaluation of tritium inventory in breeding blanket. The irradiation effects on the prosity change and thermal conductivity are important to understand the tritium recovery and cracking propagation of sintered Li_2O, respectively. Up to this time some studies on tritium recovery have been performed. A few experiments of small-scale in-situ recovery have been tested recently. However, data on irradiated Li_2O are not sufficient at present. Further experiments are necessary under high irradiation fluence.

The minimum operating temperature of Li_2O is confirmed at about 400°C, but the maximum operating temperature depends on design. High temperature is very attractive from a thermo-hydraulic point of view. Further irradiation tests are needed stringently.

The blanket configuration will be needed to be revised in order to avoid the cracking and to accommodata the change of thermal conductivity.

The pebble-packed type blanket concept is potentially a strong candidate. In this blanket structure, when beryllium pebble is used in homogeneous mixture with breeding material pebble, the obtainable tritium breeding ratio will be increased remarkably.

(2) Shield

There are considerable activities in the R & D of shielding and radioactivity for fusion reactor in Japan by using D-T neutron source facilities. They are 1) experiments on fast neutron streaming through duct and activation of various samples at the FNS facility of JAERI and 2) experiments on the leakage spectra from various shielding materials and sky-shine effect at the OKTAVIAN of Osaka University.

Two kinds of streaming experiments were carried out by utilizing experimental ports prepared in the shield wall of FNS target rooms. One experiment is on a straight port of 42 cm diameter facing to the rotating target. The detailed spatial distributions of fast neutron were measured across the streaming beam as well as the neutron spectra at selected locations of the traverses. The results were compared with the calculation by DOT3.5 transport code. The other is an experiment on a set of parallel small-diameter long holes. The axial distribution of fast neutrons was measured in each hole into which the source neutron entered with different incident angles from 0 to 6 degrees. In both cases, the detector was a small-sized NE 213 spherical spectrometer.

Measurements of induced activities in 316 type stainless steel samples were performed to verify the THIDA code by using the FNS facility. It was demonstrated that the calculation can predict the total gamma doses within 15 %, though there were some disagreement in the intensities of individual gamma-ray peaks. Activation measurements on some structural materials and concrete samples are in progress.

Leakage neutron spectra from various shielding materials were measured by means of time-of-flight methods at the OKTAVIAN as benchmark experiments to assess neutron cross section data and method for shielding calculation of D-T neutron.

High intensity neutron source could enable the experimental evaluation of neutron streaming problems combined with deep penetration i.e. to evaluate neutron flux consisting comparable amount of neutrons streaming through a small slit or duct and those penetrating through very thick shield to examine the accuracy of the calculations in the design study. It also enable to measure nuclear heating more directly and accurately.

(3) Tritium

Main research areas in JAERI related to tritium technology for fusion at present, are forcused on the field of tritium processing, safe handling, tritium production, and health physics. Basic technologies for these areas will be developed with the next half decade. The TPL (Tritium Process Laboratory) in JAERI will be a key facility in basic tritium technology development.

Component studies for fuel cleanup, have been carried out, and devoted both to palladium diffusers for separating hydrogen isotopes from all other impurities and to ceramic electrolysis cell for decomposing tritiated water vapor with very low tritium inventory. In the former, the permeation characteristics of protium and deuterium, and the effects of the presence of impurities on hydrogen isotope permeation have been studied. In the latter, the basic cell performance has been obtained by using ordinary water vapor. Recently, the effect of tritium on these components has been investigated at TSTA facility of Los Alamos Nation Laboratory under collaboration between US-DOE and JAERI.

In the development of tritium production technology, extraction and purification of tritium gas produced in neutron irradiated $^{6}LiAl$ target have been carried out. The present handling level is 50 ~ 100 Ci. It will be elevated up to approximately one order of magnitude near future.

In the study of ceramic lithium compunds as breeding materil, the preparation and the measurement of thermochemical properties of lithium oxide pellet have been successively performed. And the neutron irradiation experiments for in-situ tritium behavior measurement was initiated.

In tritium monitoring activities, monitoring services such as area monitoring and urine analysis have been performed, and the development of tritium concentration measurement by bremsstrahlung is being conducted.

Tritium safe handling (as well as tritium processing) in fusion facility is strongly dependent on tritium transfer mechanism of fusion device. The permeation and trap of tritium in structural and breeding materials must be fully studied. Development of tritium barriers for permeation is needed to reduce tritium permeation rate to the working area and to the environment. The other problems on the tritium safe containment such as adsorption and desorption of tritium at the reactor room wall surface is to be investigated.

Tritium oxide is assessed to be much more toxic than elemental tritium. So the conversion of tritium in atmosphere to oxide should be intensively investigated especially on kinetics. And biological toxicity of tritiated species should be also well understood.

(4) Safety

The code, criteria and guideline for LWR, which are reviewed before its construction and operation have been already developed and are being improved. Up to now those for fusion reactor system does not exist.

New criteria appropriate for the fusion system are required, concerning with plasma core, magnet system, fuel cycle, reactor building and so on. However, some of those for LWR may be applicable to the fusion reactor system with or without modification. Since the purpose of the siting criteria is the protection of the public from the radiation hazard and it should not be dependent on the kind of the nuclear power system, it can be the typical one which is applicable to the fusion power system.

Tritium concentration level in the primary coolant strongly affects the size of detritiation system. The numerical code TRIP based on Fickian diffusion equation analyzes the transient-state hydrogen isotopes migrations. Comparing a pulsed mode operation with steady state operation mode tritium migration during the dwell time is found to be negligibly slow, and 4.1 years continuous operation corresponds to whole INTOR mission period.

The permeation through the outboard first wall is no greater than 1 Ci/day at the end of INTOR mission even if the thinner wall corresponding to the end of life is used. The molecular sticking coefficient is the most critical parameter which has strong effects on the magnitude of tritium permeation.

There are some accident analysis codes which deal with cooling pipe rupture accident in a tritium producing blanket, magnet accident, tritium system accident and cryogenic system accident. They are now being improved.

9. Design modification

The conceptual design concept for INTOR was developed in the Phase One workshop. In the Phase Two A, Part 1 and 2 workshop, we have studied critical technical issues and have also assessed scientific and technical data bases. Based on those results, the INTOR design have been modified to upgrade the design concept. The major modification items are related to plasma beta value, plasma operation scenario, reactor size reduction, neutron fluence, tritium producing blanket, and implementation of active control coils. The vertical view of modified INTOR is shown in Fig. 9-1.

Reduction of a gap between the design value and the predicted beta limit

The total average beta value (5.6 %) of the present INTOR design is rather optimistic and somewhat beyond the critical beta limit (3.46 %) predicted from the empirical beta limit scaling ($3.5I_p$[MA]/a[m]B_T[T]), which is derived from recent experimental and theoretical studies, and most of experimental data are below this limit. Narrowing down the gap between the design beta value and the predicted beta limit have been included in the design modification. One potential way for reduction of the beta gap is the increase of plasma current and the decrease of plasma major radius, based on the empirical beta scaling. Another possible way is the reduction of non-DT contributions in addition to the fuel DT beta value (4.57 %), 45 % of which is alloted to the non-DT contributions at present.

The reduction of the plasma major radius have been achieved by the following potential engineering improvements. The first is the reduction of the inboard shield by 10 cm. The second is the increment of the maximum experience field of poloidal field coils, which use Nb_3Sn instead of NbTi. The last improvement is to increase current densities of toroidal (30 A/mm^2) and poloidal (25 A/mm^2) field coils. Those engineering improvements make the reduction of 0.3 m in the major radius feasible. The reduction of the excess of the average total beta value is accomplished by the increase of the plasma current, from 6.4 MA to 7.5 MA and the reduction of the plasma major radius, from 5.3 m to 5.0 m. It raises the beta limit (4.4 %) predicted by the empirical scaling. The other is the reduction of the additional beta value, which should be provided for impurities, high energy particles and thermalized helium particles, in addition to the beta value due to fuel DT ions. The additional beta value is chosen to be 30% of the DT fuel beta value (4.58 %) instead of 45 %. Then the total beta value amounts to 5.92 %, which increases from the reference value of 5.6 %.

Based on the above considerations, the simple plasma analysis numerical code yields the main plasma parameters, as shown in Table 9.1. The plasma current is selected to be 7.5 MA, which corresponds to 1.7 of the safety factor, taking account of ellongation, and could be over 2, when the toroidal effects is included. The total beta value increases up to 5.92% from 5.6%. The critical beta limit predicted by the empirical scaling also increases due to the enhanced plasma current. Then, ratio of the total beta value to the critical one is reduced to 1.34 from 1.62. The excess of the total beta value beyond the critical one is also reduced to 1.35% from 2.14%.

Operation scenario

In the present INTOR design, the plasma current is inductively driven by OH coils throughout the whole pulse of more than 200 s, including start-up, burn, and shut-down. In the design modification, the increase in the plasma current and the reduction of the plasma major radius, retaining the present inductive volt second, are incorporated to narrow the beta gap betwwen the design value and the beta limit. It reqiuires reconsideration of the present operation scenario.

Remarkable progresses have been made experimentally and theoretically in non-inductive current drive with a LH wave, and the further progress may be expected in this area. Based on analyses and evaluations on this issue, the non-inductive current ramp-up and recharging scenario with the LH wave is incorporated in the design modification to resolve the estimated problem about the required volt second and to gain engineering benefits associated with the non-inductive scenario.

(Physics considerations)

The modified operation scenario with non-inductive current ramp-up and transformer recharge with a LH wave is shown in Fig. 9.2. The operation scenario consists of seven phases; (A) start-up phase including a current ramp-up to 5.7 MA, (B) heating phase to ignition, (C) burn phase, (D) cooling phase for recharging or shutdown, (E) recharging phase for OH coils, (G) shutdown phase, and (H) dwell phase.

Table 9.1 Modified main plasma parameters

Plasma major radius, R_p(m)	5.0
Plasma radius, a(m)/b(m)	1.2/1.92
Aspect ratio, A	4.167
Elongation, K	1.6
Triangularity, δ	> 0.2
Average ion temperature, $\langle T_i \rangle$ (keV)	10
Average ion density, $\langle n_i \rangle$ (10^{20} m^{-3})	1.4
Total beta, β_t (%)	5.92
Fuel beta, β_f (%)	4.57
Plasma current, I_p (MA)	7.5
Safety factor, q_I	1.7
Toroidal field, B_T (T)	4.96
Thermonuclear power, P_{th} (MW)	580
Neutron wall load, P_n (MW/m^2)	1.24

At the biginning of the start-up phase, plasma are produced and heated with an assist of ECRF heating with 10 MW, and plasmas are brought to a parameter region with around 3×10^{18} m^{-3} in densities amd 1-2 keV in temperatures. Such a low-density plasma carry well its current driven by a LH wave. Based on analyses on a current ramp-up scenario, a ramp-up time is specified $\sim$100 s, and during this period the plasma current increased up to 5.7 MA by the LH wave with a power level of 10 MW.

In the heating phase to ignition, plasmas are heated by an ICRF wave of 50 MW, and temperatures and densities are increased to the specified level of the burn phase. The plasma current is also increased from 5.7 MA to 7.5 MA inductively instead of rf drive, because of significant decrease of rf current drive efficiency in high density plasmas. The heating time is $\sim$20 s. An initial goal of a burn time is more than 1000 s, which is inductively drived. The cooling phase is an inverse process of the heating phase. The cooling time is $\sim$20 s. The prolonged cooling time may require temperature control with the ICRF wave, otherwise temperatures could drop with the shorter time of an order of confinement time. In the cooling phase, the plasma current decreased to from 7.5 MA to 5.7 MA inductively.

In the recharge phase, OH coils are recharged, while the plasma current is hold to 5.7 MA by the LH wave in plasmas with densities of around 3×10^{18} m^{-3} and temeratures of 1-2 keV. The recharging time of $\sim$200 s is also evaluated based on analyses of transformer recharge by the LH wave. In a quasi-steady operation, four phases from (B) to (E) are repeated.

(Engineering benefits)

Several engineering benefits are expected associated with the plasma current ramp up by RF instead of OH coils, that is, volt second saving, decrease of AC loss in superconducting coil system and reduction of requirement for power supply.

-Volt second saving-

In the conventional inductive current ramp up scenario the most part of volt second delivered by PF coil is consumed for plasma initiation and current ramp-up leaving a small amount of volt second for the burning phase. When the plasma current is ramped up by RF wave injection, most of the volt second can be used for burning phase leading to a longer pulse or smaller OH coil bore then smaller reactor size.

Magnetic field analyses, howevver, found some problems of superposing magnetic fields by divertor coil current and plasma current on the OH coil near divertor coil at the begining of the burn phase. This is the disadvantage inherent to the RF ramp-up scenario. The burn time of 957 s is obtained for the burn phase plasma current of 6.4 MA. When we increase the plasma current to 7.5 MA in order to mitigate the beta problem, 509 s of burn time is obtained. Since our RF coil system design for INTOR is not fully optimized, it should be possible to extend burn time to some extent by selecting proper division and location of divertor coils. Anyway there is certain advantage associated with RF current ramp up in extending burn time or reducing reactor size.

-AC loss-

The large AC loss induced in the TF and RF coil systems was a big problem in the reference INTOR design with conventional inductive current ramp-up scenario. Even with the large number of electric breaks in the support structure, which leads to the concern about the structural integrity of the supports, the total cycle averaged AC loss exceeds 100 kW. In the case of RF current ramp up, current rise can be greatly prolonged ($\sim$ 100 sec) and AC loss is dramatically reduced without significant structural problems in the support system. The result of AC loss calculation shows that total cycle averaged AC loss is about 4.3 kW. This is the great advantage of the RF ramp-up scenario.

-Cyclic Stress on the TF coil-

When quasi-steady operation mode is adopted as well as current ramp up by RF, we have further possible advantage that the fatigue problem of TF coil support can be greatly mitigated. The difficulties for supporting the superconducting TF coil of large tokamak like INTOR are mainly caused by the overturning force which results from the interaction of the TF coil current and the equilibrium field. In the pulsed operation tokamak, this force acts cyclically on TF coils. The TF coil structural design criteria include conventional (primary) stress limits in addition to limits established for stress amplitude based on fatigue life consideration. It must be expected that the stress amplitude can be reduced considerably by introducing the quasi-steady state operation. Analyses on the overturning force indicate that the amplitude of the overturning force can be reduced by sustaining the plasma current in OH coil recharging phase at lower value than the burning plasma current.

-Power supply capacity-

Typical load pattern of PF coil power supply for the case of conventional inductive current ramp-up scenario shows that peak power load appears at the end of plasma current ramp-up phase (t=5 s). At this time, apparent power for PF-coil power supply becomes as $\sim$ 2000 MVA. By adopting RF current-ramp up scenario and extend the ramp-up duration to $\sim$ 100 s power load at the end of current ramp up phase can be greatly reduced ($\sim$ 600 MVA). However since there is another peak ($\sim$ 1400 MVA) at the end of heating phase, some effort is required to reduce this peak. By extending heating phase duration and selecting proper plasma current level at the end of current ramp-up phase this peak can be reduced to about 1000 MVA. Since longer heating time requires larger power supply capacity for heating system, carefull trade-off study is necessary. Our preliminary study which compares 6 s and 20 s of heating phase duration shows that the latter heating phase duration is preferable.

Reactor size reduction

In order to reduce reactor size the following engineering improvements are implemented. The first is the reduction of the inboard shield by 10 cm. The second is the increment of the maximum experience field of poloidal field coils, which use Nb_3Sn instead of NbTi. The last improvement is to increase current densities of toroidal (30 A/mm^2) and poloidal (25 A/mm^2) field coils. Those engineering improvements make the reduction of 0.3 m in the major radius

feasible. The inboard shield thickness is reduced by changing shield criterion for the allowable nuclear heating in TFC from 5 kW to 15 kW and optimizing shield composition. The composition of 85% stainless steel and 15% water is selected as the optimum point.

The increase of TF coil current density from 25 to 30 A/mm^2 and the maximum allowable PF coil field from 8 to 10 T resulted in the reduction of TF coil thickness by 10 cm and OH coil bore by 10 cm, respectively. These engineering modification resulted in the 0.3 m of plasma major radius reduction. Both the reduction of the main radius 5.3 m to 5.0 m and the reduction of cross section of TF coil contribute to the reduction of the reactor structure size (diameter of the belljar) by 1 m.

As for the vertical dimension of the reactor, the impact of the choice of impurity control system is considerable. As a reference design, the short channel type configuration of the divertor is adopted in order to reduce the reactor size. The maximum heat load on divertor plate of short channel concept is about 5 MW/m^2. This design condition is very severe from the view point of the thermal stress. If the permissible level of the maximum heat load 2 MW/m^2 is adopted, the increasing length of divertor plate in horizontal direction leads to the increase in TF coil bore and the short channel divertor is not recommendable.

Tritium producing blanket

In the previous blanket design studies for INTOR, continuous tritium recovery scenario has been proposed based on economic and tritium availability considerations. However, design requirements associated with continuous tritium recovery such as the precise temperature control of breeder, lead to complexity of blanket design. A improvement of the simplicity and reliability is desired for tritium producing blanket. A batch-type tritium recovery scenario is proposed as a solution of simple and reliable tritium producing blanket, and design feasibility studies have been performed.

The design philosophies adopted for accomplishing the simplicity and reliability are as follows:

(i) Batch-type tritium recovery scenario is adopted to simplify the temperature control mechanism of breeder.
(ii) To provide high reliability performance of shell effect, copper alloy (Cu-Be-Ni) which offers possible advantage over pure copper in the area of radiation damage resistance is used as a shell conductor material.
(iii) Low temperature helium gas is selected as the coolant to avoid coolant/breeder reaction in accident.
(iv) To achieve the high tritium breeding ratio, lithium oxide (Li_2O) and beryllium are used as a tritium breeding material and a neutron multiplier, respectively.

There are two major factors that reduces simplicity and reliability of blanket. One is the temperature control requirement of breeder (ex. 400 1000 °C for Li_2O) to ensure continuous in-situ tritium recovery during reactor operation. This factor imposes installation of thermal insulation gap to provide temperature difference between breeder and coolant tube. The other is the addition of neutron multiplier and shell conductor for passive plasma stabilization with their cooling mechanism and support structure. Application

of beryllium plate potentialy be a candidate, since it can be used as both neutron multiplier and shell conductor. However, limited ductility of beryllium relative to other structural materials imposes some constraints on design, fabrication and reliability of the shell structure.

For the above reasons, design approaches in this selection study are focussed on simple and reliable blanket concept in the area of temperature control mechanism and neutron multiplier/shell conductor. Elimination of thermal gap around cooling tube is essential for simple design of blanket. If continuous in-situ tritium recovery is a design requirement of blanket, refractory metals must be developed for the structure materials. But if the continuous in-situ recovery of bred tritium is excluded from blanket design requirements, stainless steel (or PCA), that has most developed data base for nuclear application, can be used as structure material.

There are three options available for basic thermal hydraulic design of batch recovery blankets: (i) Water-cooled blanket, (ii) Directly-helium-cooled blanket, and (iii) Indirectly-helium-cooled blanket. Of these three concepts, indirectly-helium-cooled blanket appears most attractive and selected as the reference of the present study, because of its high potential of tritium breeding performance and easiness of periodic tritium recovery.

Fluence

Materials tests is the one of the INTOR operation purpose. The minimum fluence required for a structural material irradiation test is said to be 3 MWY/m^2. And considering fusion reactor development schedule, the irradiation test duration should not be too long. It seems that around 10 years may be the proper duration. When we want 6.6 MWY/m^2 of fluence during 10 years operation (0.66 MWY/m^2/Y), about 0.8 of tritium breeding ratio is required since the tritium procurment available in near future does not seem to exceed 3 kg/Y. The breeding ratio of 0.8 requires installation of breeding blanket on the inboard side of reactor making reactor size increased. The fluence of 3 MWY/m^2 in 10 years can be achievable with the tritium breeding ratio of 0.6. Then the fluence of 3 MWY/m^2 is recommendable from above consideration and the finding that the fluence reduction is very effective in decreasing INTOR cost as shown in the cost benefit analysis in Phase IIA Part I.

Implementation of active control coil

Through the Phase IIA Part 1 and 2 the plasma vertical position control is discussed as one of the critical issues mainly from the viewpoint of electromagnetics. However, active control coil, which is essential component for stabilizing the plasma, has not been implemented into the mechanical configuration of the reference INTOR. The following items should be taken into consideration to determine the location of installation of the active control coil which produces the horizontal magnetic field constituent.

(a) Active coil should be installed in the location where the magnetic field of horizontal constituent can be generated efficiently and the power supply capacity required is small enough.
(b) Installation of the active control coil should be easy and the structure supporting the active control coil should be simple.
(c) Radiation damage should be low enough.
(d) Assembly and disassembly procedures should be simple and easy.

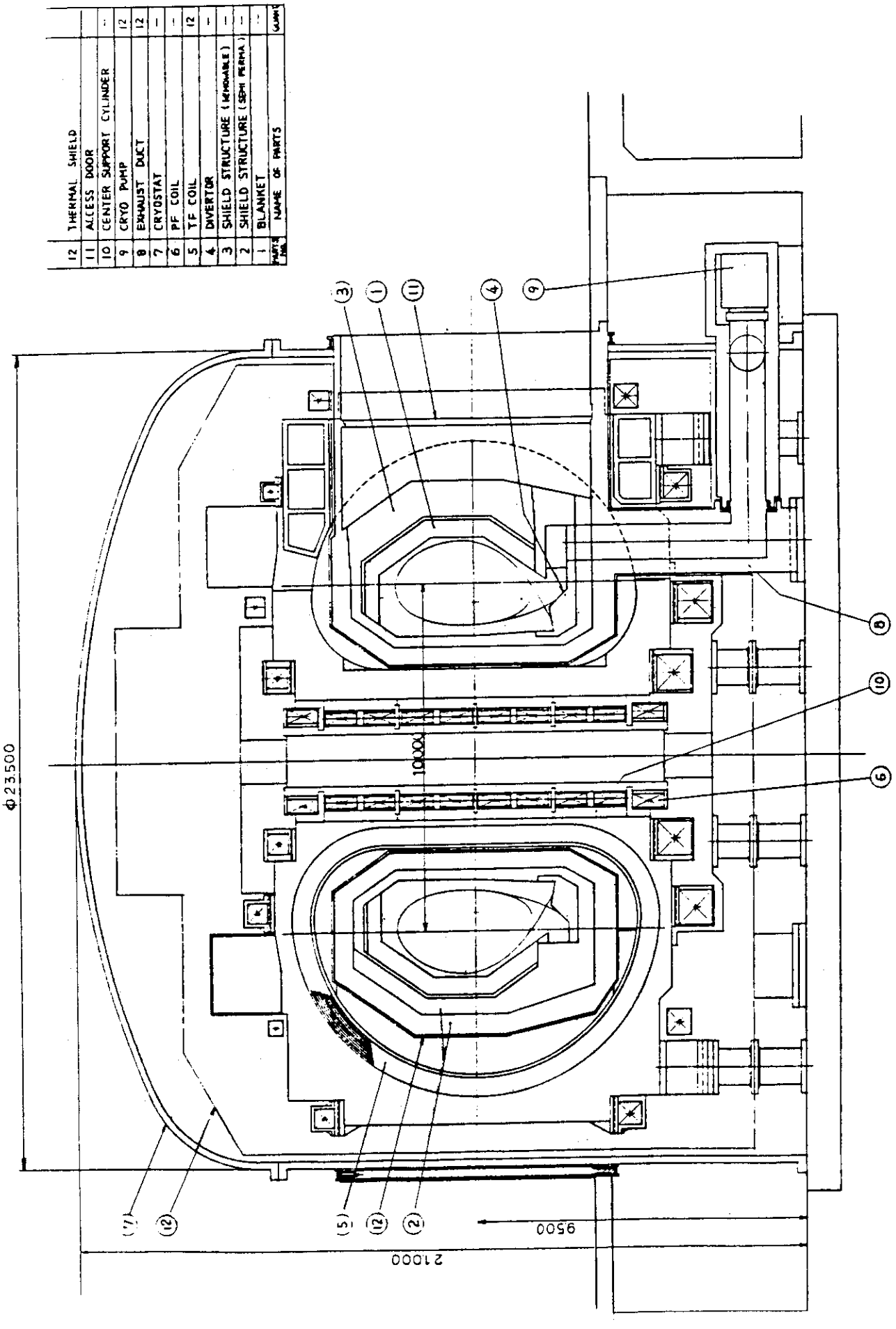

Fig. 9-1 Vertical View of Modified INTOR

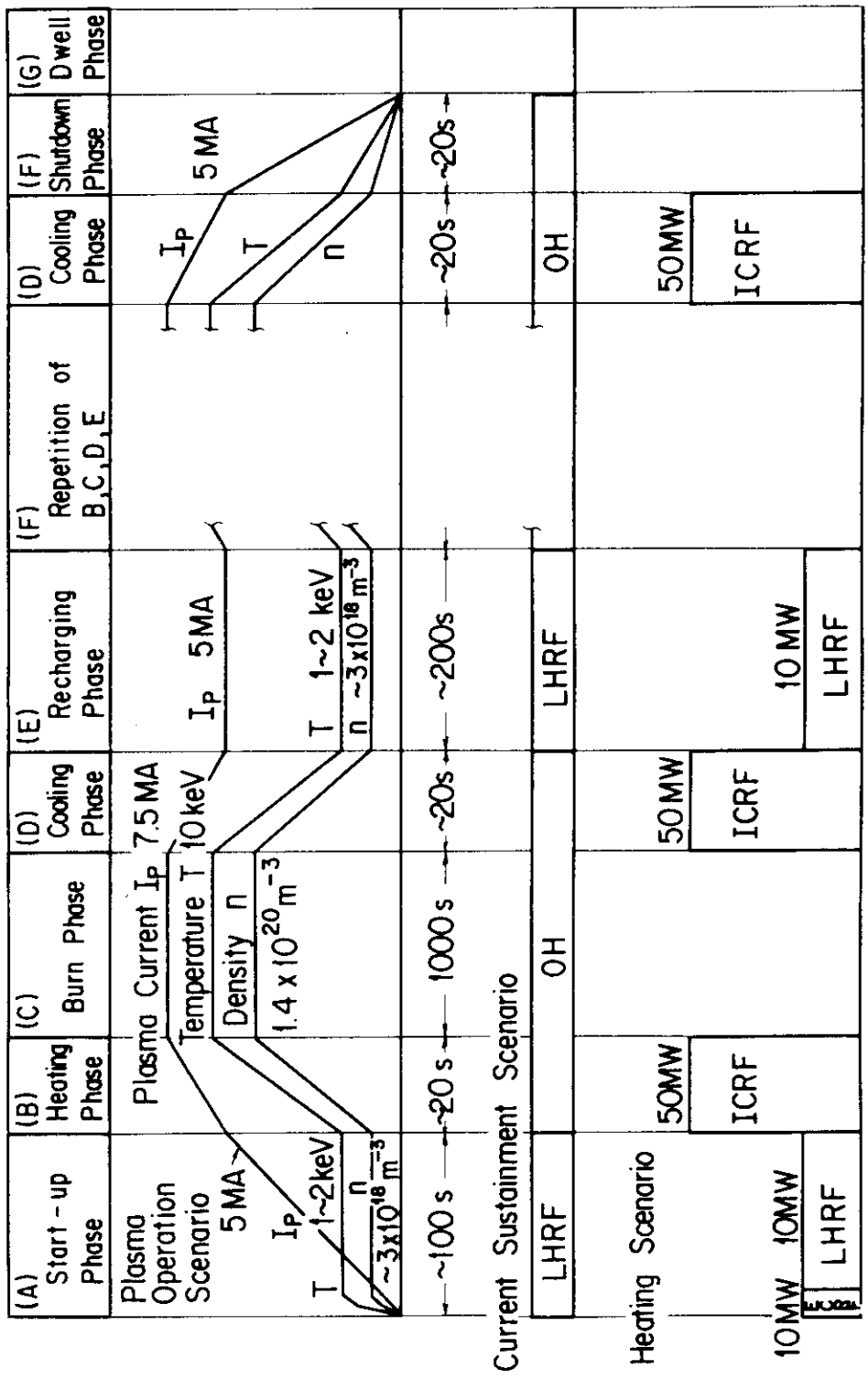

Fig. 9.2 Modified INTOR operation scenario